In-car particulate matter exposure across ten global cities

Prashant Kumar [a,b,*], Sarkawt Hama [a], Thiago Nogueira [a,c,d], Rana Alaa Abbass [a], Veronika S. Brand [a,d],
Maria de Fatima Andrade [d], Araya Asfaw [e], Kosar Hama Aziz [f], Shi-Jie Cao [a,g,h], Ahmed El-Gendy [i], Shariful Islam [j],
Farah Jeba [j], Mukesh Khare [k], Simon Henry Mamuya [l], Jenny Martinez [a,m], Ming-Rui Meng [h], Lidia Morawska [a,n],
Adamson S. Muula [o], S.M. Shiva Nagendra [p], Aiwerasia Vera Ngowi [l], Khalid Omer [f], Yris Olaya [m],
Philip Osano [q], Abdus Salam [j]

[a] Global Centre for Clean Air Research (GCARE), Department of Civil and Environmental Engineering, Faculty of Engineering and Physical Sciences, University of Surrey, Guildford GU2 7XH, United Kingdom
[b] Department of Civil, Structural & Environmental Engineering, Trinity College Dublin, Dublin, Ireland
[c] Departamento de Saúde Ambiental – Faculdade de Saúde Pública, Universidade de São Paulo, São Paulo, Brazil
[d] Departamento de Ciências Atmosféricas – Instituto de Astronomia, Geofísica e Ciências Atmosféricas — IAG, Universidade de São Paulo, São Paulo, Brazil
[e] Physics Department, Addis Ababa University, Ethiopia
[f] Department of Chemistry, College of Science, University of Sulaimani, Kurdistan Region, Iraq
[g] School of Architecture, Southeast University, Nanjing 21009, China
[h] Academy of Building Energy Efficiency, School of Civil Engineering, Guangzhou University, Guangzhou 510006, China
[i] Department of Construction Engineering, School of Sciences and Engineering, The American University in Cairo, New Cairo 11835, Egypt
[j] Department of Chemistry, University of Dhaka, Dhaka 1000, Bangladesh
[k] Department of Civil Engineering, Indian Institute of Technology Delhi, India
[l] Department of Environmental and Occupational Health, Muhimbili University of Health and Allied Sciences, Dar-es-Salaam, Tanzania
[m] Universidad Nacional de Colombia, Colombia
[n] International Laboratory for Air Quality and Health, Queensland University of Technology, Brisbane, Australia
[o] University of Malawi, Malawi
[p] Department of Civil Engineering, Indian Institute of Technology Madras, India
[q] Stockholm Environment Institute, Nairobi, Kenya

HIGHLIGHTS

- Particulate matter (PM) exposure in cars was measured across ten global cities.
- Windows-open scenarios resulted in the highest PM_{10} and $PM_{2.5}$ concentrations.
- PM exposure was significantly higher during morning-peak hours in most cities.
- Recirculation showed up to 80% less in-car $PM_{2.5}$ compared to windows-open.
- Off-peak trips showed up to 73% less $PM_{2.5}$ exposure compared to morning-peak hours.

GRAPHICAL ABSTRACT
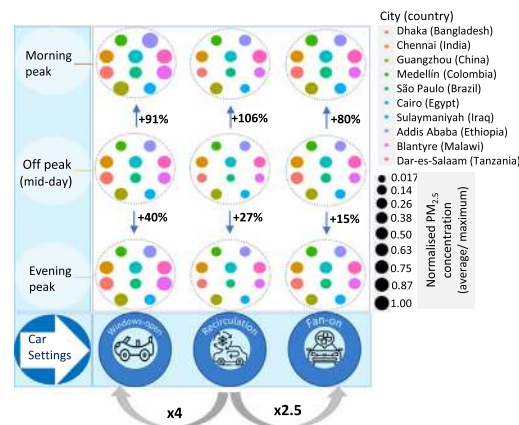
* Corresponding author at: Global Centre for Clean Air Research (GCARE), Department of Civil and Environmental Engineering, Faculty of Engineering and Physical Sciences, University of Surrey, Guildford GU2 7XH, United Kingdom.
E-mail address: p.kumar@surrey.ac.uk (P. Kumar).

ARTICLE INFO

ABSTRACT

Cars are a commuting lifeline worldwide, despite contributing significantly to air pollution. This is the first global assessment on air pollution exposure in cars across ten cities: Dhaka (Bangladesh); Chennai (India); Guangzhou (China); Medellín (Colombia); São Paulo (Brazil); Cairo (Egypt); Sulaymaniyah (Iraq); Addis Ababa (Ethiopia); Blantyre (Malawi); and Dar-es-Salaam (Tanzania). Portable laser particle counters were used to develop a proxy of car-user exposure profiles and analyse the factors affecting particulate matter ≤2.5 μm (PM$_{2.5}$; fine fraction) and ≤10 μm (PM$_{2.5-10}$; coarse fraction). Measurements were carried out during morning, off- and evening-peak hours under windows-open and windows-closed (fan-on and recirculation) conditions on predefined routes. For all cities, PM$_{2.5}$ and PM$_{10}$ concentrations were highest during windows-open, followed by fan-on and recirculation. Compared with recirculation, PM$_{2.5}$ and PM$_{10}$ were higher by up to 589% (Blantyre) and 1020% (São Paulo), during windows-open and higher by up to 385% (São Paulo) and 390% (São Paulo) during fan-on, respectively. Coarse particles dominated the PM fraction during windows-open while fine particles dominated during fan-on and recirculation, indicating filter effectiveness in removing coarse particles and a need for filters that limit the ingress of fine particles. Spatial variation analysis during windows-open showed that pollution hotspots make up to a third of the total route-length. PM$_{2.5}$ exposure for windows-open during off-peak hours was 91% and 40% less than morning and evening peak hours, respectively. Across cities, determinants of relatively high personal exposure doses included lower car speeds, temporally longer journeys, and higher in-car concentrations. It was also concluded that car-users in the least affluent cities experienced disproportionately higher in-car PM$_{2.5}$ exposures. Cities were classified into three groups according to low, intermediate and high levels of PM exposure to car commuters, allowing to draw similarities and highlight best practices.

1. Introduction

Particulate matter (PM) exposure causes a global loss in life expectancy of almost three years (Lelieveld et al., 2020) and results in more than seven million premature deaths annually owing to household and ambient air pollution (WHO, 2016). Acute and chronic human exposure to ambient PM exposes receptors to high-risk diseases including asthma, lung cancer, heart disease, stroke, type II diabetes, dementia, and loss of cognitive functions (Brauer et al., 2008; HEI, 2010; Loxham and Nieuwenhuijsen, 2019). PM pollution also damages the climate and ecosystems (Landrigan et al., 2018), urban settlements (Oliveira et al., 2019) and built infrastructure (Kumar and Imam, 2013).

The focus of this work is on particles with an aerodynamic diameter ≤2.5 μm (PM$_{2.5}$) and ≤10 μm (PM$_{10}$). PM is composed of solid particles and liquid droplets containing acids, organic chemicals, metals, soil or dust (Anderson et al., 2012). PM$_{2.5}$ can remain suspended in the air for several weeks and be transported over great distances (WHO, 2006; Kollanus et al., 2017), and can penetrate the human body through the respiratory system, to the blood circulatory system (Kioumourtzoglou et al., 2016). The coarse fraction (PM$_{2.5-10}$) usually contains crystal materials and fugitive dust sourced from the resuspension of road dust and construction sites; they can easily deposit and thus travel for short distances (WHO, 2006). Both fine and coarse particles are important indicators of exhaust and non-exhaust contributions in assessment of PM exposure in on-road car environments.

Exposure to air pollution is a function of the concentration of pollutants in a certain space and the time spent by inhabitants in that space (Cepeda et al., 2017; HEI, 2010). Commuters' exposure to concentrations of traffic-related air pollutants, including PM$_{2.5}$, are generally higher due to their proximity to less dispersed emissions from mobile sources (Kumar et al., 2018a). The adverse health impacts of traffic-related air pollution can even be observed within 200 m of busy roadways and highways (Brugge et al., 2007; HEI, 2010). On-road vehicle commuters are consequently front line recipients of pollutant concentrations that often exceed ambient air quality standards (Cepeda et al., 2017; Pant and Harrison, 2013).

Road traffic significantly contributes to commuters' exposure to PM, and recent studies have focused on pollutant exposures in both motorised (bus, taxi, car and motorcycle) and active (walking and cycling) modes (Betancourt et al., 2017; Do et al., 2014; Yang et al., 2015; Panis et al., 2010). Global vehicle counts have been increasing at a rate of 30–50% over the last decade in Africa, Asia, the Middle-East

and Latin America (Davis and Boundy, 2016), and with global car counts projected to reach two billion by 2040 (Smith, 2016). The mean concentrations of coarse particles are typically lowest for car-users (windows-closed with air conditioning on) and highest for bus passengers among bus, walk, cycle and car microenvironments, whereas fine particle concentrations are typically highest for car-users with windows-open (Kumar et al., 2018b). For example, PM$_{2.5}$ concentrations in Arnhem (Zuurbier et al., 2010) were higher in cars versus buses when both environments were adjusted to windows-closed setting. Furthermore, a considerably high mass fraction of fine particles (PM$_{2.5}$/PM$_{10}$ ≈ 0.90) was reported for windows-closed cars, with air conditioning and air intake from outside, when compared with bus, cycling and walking (Kumar et al., 2018b). Traffic intersections expose car commuters to ~25% of the total commuting exposure despite spending only 2% of commuting time at signalised traffic intersections (Goel and Kumar, 2015). There are several factors that affect variability in commuters' pollutant exposure, including travel times and days (i.e. peak and off-peak hours, weekday and weekend), travel modes (i.e. the transport system, technology) and characteristics of the path travelled (i.e. street configuration and geometry, micrometeorology, wind speed or traffic) (Onat et al., 2019; Betancourt et al., 2017; Yang et al., 2015; Dons et al., 2012). For example, the accumulated air pollution exposure caused by traffic ranged 54–67% lower for low exposure routes when compared to high exposure routes and 5–20% lower when travelling outside the rush hour (Hertel et al., 2008). Seasonal variations were captured in Hong Kong, where commuters were exposed to significantly higher PM$_{2.5}$ concentrations in winter than in summer (X. Li et al., 2017). Other studies explored the impact of different car settings in comparison to other modes of transport, where recirculation setting resulted in a reduction of in-car PM$_{2.5}$ concentration, of up to 75% in a field study in Sacramento, California (Ham et al., 2017) when compared to windows-open setting, and another study exhibiting the lowest PM$_{2.5}$ average exposures in Istanbul, Turkey (Onat et al., 2019) during recirculation setting.

A holistic (Kumar et al., 2018a) and a specific (Table S1) review of the literature suggests that in-car exposure studies have usually focused on one city or country, restricting opportunities for generalisation across numerous cities. Moreover, a limited number of in-car exposure campaigns have been carried out in the studied cities and the available data is usually inconsistent and for short durations, using varied sampling methodology (Table S1). The derived conclusions from the studies listed in Table S1 indicate that PM pollution in cities of interest

consistently exceeds national and international standards. Correlations are also drawn between PM pollution and traffic congestion and the impact of seasonal and temporal variations on pollution levels is observed. The cities conform with the international trend of reliance on private vehicles as a preferred means of transport due to its flexibility and prevalent affordability. Overall, almost none of the studies focus on PM emission exposure in cars to investigate the impact of different car settings and times of the day. For the first time, the current study has produced an internationally comparable dataset, using a unified methodology to report and compare exposure to $PM_{2.5}$ and PM_{10} in 10 different cities across the world. The chosen cities cover a broad geographical spectrum, from Asia to the Middle East and Africa to South America (Section 2.2). These represent a diverse range of developing countries across these heavily populated continents where the issue of traffic congestion and its adverse impact on human health are prevalent. The lack of car exposure studies is also evident in these cities (Table S1). The study incorporates three (São Paulo, Cairo and Dhaka) out of the top ten most populous megacities globally, which suffer from the consequences of traffic congestion (United Nations, 2018). Medellín, Dar-es-Salaam, Sulaymaniyah, Guangzhou and Blantyre also face challenges of poor air quality caused by road transport among other pollution sources (AMVA, 2019; Wang et al., 2018; Mapoma et al., 2014; Petkova et al., 2013). These cities all lack personal exposure studies to assess and elucidate exposure under different car settings (Table S1).

Quantification of personal exposure to different PM fractions inside car microenvironments is an essential first step towards identifying the most effective strategies for reducing exposure (Kumar et al., 2018b; Rivas et al., 2017). As part of this study, different global cities that suffer the consequences of a common international issue were brought together in one experiment, filling a worldwide knowledge gap. The aim was to assess measured $PM_{2.5}$ and PM_{10} concentrations inside often-used vehicles and investigate differences between three car settings – windows-open, fan-on (windows-closed) and recirculation (windows-closed) – and different daytime periods (morning and evening peak hours and midday off-peak hours), in order to identify the main drivers of exposure during typical commuting. Common methods of data collection and analysis (Section 2) were employed across all cities to support sound observations, constructive conclusions and holistic recommendations. The overall goal of this work was to understand the underlying factors in exposure to fine and coarse particulate matter in different cities, test the feasibility of using affordable portable pollution monitoring instruments, develop preliminary exposure profiles of car-users, and finally discuss exposure mitigation strategies. The scale and depth of this study is unprecedented, enabling a comprehensive comparison that provides a perspective on national conditions in reference to a global scientific analysis.

2. Methodology

2.1. Study design

PM concentrations within the car were evaluated in 10 cities from four major regions of the world (Section 2.2). Measurements were undertaken under three different car settings: (i) windows open with fan/recirculation off (windows-open); (ii) windows closed with fan on (fan-on); and (iii) windows closed with recirculation mode on (rec). All runs were carried out on weekdays and at three different time periods for each car setting: morning peak hours (MP), off-peak hours (OP), and evening peak hours (EP). A minimum of three runs and a maximum of 10 runs were made under each setting (Section 2.3). A total of 540 runs were carried out, taking 30,443 min (507 h) and covering a distance of 573 km across all cities (Table 1). The car routes (Section 2.2) were chosen to include similar urban exposure scenarios, such as residential areas, commercial areas, heavy traffic roads and

Table 1

Summary of study details, showing the average route length and the average time taken to complete a trip in each of the three car settings. The total time taken for all trips/runs with the number of trips between brackets is also listed for all cities. The code name of cities are picked up according to the airport acronym for that city.

City (code)	Settings	Route length (km)	Average time $\pm$ SD (min)	Total time for collected data in minutes (# of trips)			
				MP	OP	EP	Total time (total # of trips)
Dhaka (DAC)	Fan-on	32.3 $\pm$ 1.5	188.1 $\pm$ 43.2	794 (5)	545 (4)	974 (4)	2310 (13)
	Rec	33.0 $\pm$ 1.7	146.2 $\pm$ 40.4	808 (6)	669 (5)	578 (4)	2055 (15)
	Open	32.4 $\pm$ 1.7	158.4 $\pm$ 63.5	1562 (11)	516 (4)	1596 (10)	3674 (25)
Chennai (CHE)	Fan-on	13.4 $\pm$ 0.5	31.1 $\pm$ 5.1	85 (3)	90 (3)	121 (3)	296 (9)
	Rec	13.5 $\pm$ 0.1	31.1 $\pm$ 2.1	91 (3)	97 (3)	115 (3)	303 (9)
	Open	13.7 $\pm$ 0.1	33.1 $\pm$ 3.3	104 (3)	92 (3)	133 (3)	329 (9)
Guangzhou (CAN)	Fan-on	24.7 $\pm$ 0.6	35.4 $\pm$ 3.1	180 (6)	237 (7)	265 (3)	682 (16)
	Rec	24.8 $\pm$ 0.2	36.4 $\pm$ 2.4	216 (6)	252 (7)	273 (7)	741 (20)
	Open	24.6 $\pm$ 0.7	34.1 $\pm$ 4.1	208 (6)	244 (7)	214 (6)	666 (19)
Medellín (MDE)	Fan-on	16.5 $\pm$ 0.2	54.3 $\pm$ 8.3	606 (11)	652 (12)	691 (10)	1949 (33)
	Rec	16.6 $\pm$ 0.2	57.3 $\pm$ 4.2	581 (10)	721 (12)	723 (10)	2025 (32)
	Open	16.6 $\pm$ 0.2	52.3 $\pm$ 3.5	576 (11)	553 (10)	711 (11)	1840 (32)
Sao Paulo (SAO)	Fan-on	12.7 $\pm$ 0.3	56.3 $\pm$ 7.1	441 (10)	588 (10)	654 (10)	1683 (30)
	Rec	12.8 $\pm$ 0.4	55.3 $\pm$ 7.2	436 (10)	587 (10)	638 (10)	1661 (30)
	Open	12.6 $\pm$ 0.3	49.4 $\pm$ 8.0	402 (10)	522 (10)	565 (10)	1489 (30)
Cairo (CAI)	Fan-on	16.1 $\pm$ 0.1	46.4 $\pm$ 8.1	260 (7)	176 (4)	291 (5)	727 (16)
	Rec	16.2 $\pm$ 0.1	46.3 $\pm$ 8.2	433 (10)	430 (10)	506 (10)	1369 (30)
	Open	16.2 $\pm$ 0.1	42 $\pm$ 8.6	314 (10)	437 (10)	511 (10)	1262 (30)
Sulaymaniyah (SUL)	Fan-on	32.3 $\pm$ 3	55.4 $\pm$ 6.3	465 (9)	369 (7)	445 (8)	1279 (24)
	Rec	33.9 $\pm$ 0.7	57.3 $\pm$ 4.4	281 (5)	369 (5)	445 (5)	835 (15)
	Open	33.1 $\pm$ 2.8	64.2 $\pm$ 8.2	451 (7)	440 (7)	367 (6)	1258 (20)
Addis Ababa (ADD)	Fan-on	10.6 $\pm$ 0.1	35.4 $\pm$ 5.4	158 (4)	103 (3)	112 (3)	373 (10)
	Rec	10.5 $\pm$ 0.1	34.5 $\pm$ 6.1	110 (3)	98 (3)	109 (3)	317 (9)
	Open	10.6 $\pm$ 0.1	36.3 $\pm$ 3.3	114 (3)	143 (4)	112 (3)	369 (10)
Blantyre (BLZ)	Fan-on	11.2 $\pm$ 2.9	33.1 $\pm$ 10.2	109 (4)	84 (3)	114 (3)	397 (10)
	Rec	10.8 $\pm$ 3.4	29.3 $\pm$ 8.5	85 (3)	82 (4)	114 (4)	281 (11)
	Open	10.9 $\pm$ 1.1	29.2 $\pm$ 5.2	197 (7)	92 (3)	93 (3)	382 (13)
Dar-es-Salaam (DAR)	Fan-on	20.4 $\pm$ 0.8	113.1 $\pm$ 5.1	305 (3)	256 (3)	493 (3)	1054 (9)
	Rec	20.2 $\pm$ 0.6	130.2 $\pm$ 14.1	263 (3)	318 (3)	520 (3)	1101 (9)
	Open	20.2 $\pm$ 1.3	133.3 $\pm$ 17.4	301 (3)	334 (3)	510 (3)	1145 (9)

Note that the average length (in km) of the route in each city (Fig. S1) is as follows: DAC (32.6 $\pm$ 1.6), CHE (13.5 $\pm$ 0.2), CAN (24.7 $\pm$ 0.5), MDE (16.6 $\pm$ 0.2), SAO (12.7 $\pm$ 0.3), CAI (16.2 $\pm$ 0.1), SUL (33.1 $\pm$ 2.2), ADD (10.6 $\pm$ 0.1), BLZ (10.9 $\pm$ 2.5) and DAR (20.3 $\pm$ 0.9).

green areas. In all cities, a route with a minimum of 10 km length was chosen, which passed through congested main roads and residential zones. The very same passenger car was employed for all runs in each city; details are presented in Supplementary Information (SI) Table S2. In the car, there were up to two non-smokers including the driver, and the PM readings were collected from the backseat to simulate car passenger exposure. The study capitalised on the advancement in affordable PM sensing technology by using Dylos monitors in all cities, giving access to novel and comparative personal exposure data (Z. Li et al., 2017; Kumar et al., 2015b ; Yu et al., 2012). Portable air quality and GPS monitors were used to measure PM concentrations and track the predefined closed route in each city. All monitors were calibrated by the manufacturer and further compared to a reference monitor prior to their deployment in all cities. Quality control measures (Section 2.5) ensured an equitable comparison between measurements in the different cities.

2.2. Description of study area and the routes

The study involved 10 cities (listed below) across four regions, namely Asia (India, Bangladesh, China), Latin America (Colombia and Brazil), Africa (Tanzania, Malawi, and Ethiopia) and the Middle-East and North Africa (Egypt and Iraq). Their locations are depicted in Fig. 1. SI presents city details (Table S3), their climatic and topographical features (Section S1), and the predominant urban PM sources in each city (Table S4). Key features of these cities are summarised Section S2.

All routes in this study were closed loops with a minimum total distance of 10 km (Table 1). Fig. S1 shows maps of the selected routes for each of the following cities: Dhaka (Bangladesh), Chennai (India) and Guangzhou (China) in Asia; Medellín (Colombia) and São Paulo (Brazil) in Latin America; Cairo (Egypt) and Sulaymaniyah (Iraq) in the Middle-East; Blantyre (Malawi), Dar-es-Salaam (Tanzania) and Addis Ababa (Ethiopia) in Africa. Route characteristics in each of these cities are summarised Section S3.

2.3. Data collection

Data collection took place between February and December 2019 and at the following three daytime periods (local time): 07:00–09:00 h (MP), 12:00–14:00 h (OP), and 17:00–19:00 h (EP). For every period, one run was performed under each of the three different settings (Section 2.1) in all cities. Readings at one-minute intervals of $PM_{2.5}$ and PM_{10} were collected with a Dylos laser particle counter (Dylos Corporation, Riverside, California, USA). In SUL, a Dylos DC1100 was used to measure the concentration of particles in two sizes: >0.5 μm and >2.5 μm. Nine Dylos DC1700 monitors (one per city) were used to measure PM mass concentrations ($PM_{2.5}$ and PM_{10}) in the remaining cities (http://www.dylosproducts.com/). A detailed quality assurance and calibration procedure for all monitors is described in Section 2.5. Since the experiment aimed to analyse commuters' exposure along a common route, measurements were carried out from Monday to Friday in all cities except SUL and CAI, where working days are Sunday to Thursday. Rainy days and extreme weather events were avoided in order to simulate typical conditions and maintain consistency across measurements for all cities. Details on data collection are summarised in Table 1. The STRAVA app (https://www.strava.com/) was used as a GPS tracker for continuous latitude and longitude recordings during car trips. Ambient temperature, relative humidity, and wind speed and direction data were collected from the nearest local airport for every run and ranged modestly within 24 ± 6 °C, $66 \pm 19\%$, and 4 ± 2 m s^{-1}, respectively (Table S5).

2.4. Data analysis

All data processing and statistical analyses were carried out using R statistical software (R Core Team, 2019) in the Open-air software package (Carslaw and Ropkins, 2012) and Igor Pro 6.7 (Wavemetrics, Portland, US). Hierarchical cluster analysis was performed, applying Ward's method to generate a dendrogram with distance based on 1-Person r (Malley et al., 2014), using Statistica software (version 13.5.0.17). ArcGIS (Esri Inc.) was used to generate route maps and to present the spatial variation of average $PM_{2.5}$ concentrations, for identifying areas in the cities with higher concentrations or hotspots (Goel and Kumar, 2014). To understand the relative intensity of hotspots in cities and to address the uncertainty introduced by trip duration variations, we calculated the 90th percentile (P90) of all one-minute averaged $PM_{2.5}$ concentration data points of all three settings to make a comparison among them (Mitchell et al., 2008) and calculated the $PM_{2.5}$ average in street segments of ~300 m. Furthermore, we calculated the percentage of the route length in each city and setting that exceeded the calculated P90 in the spatial variation of average
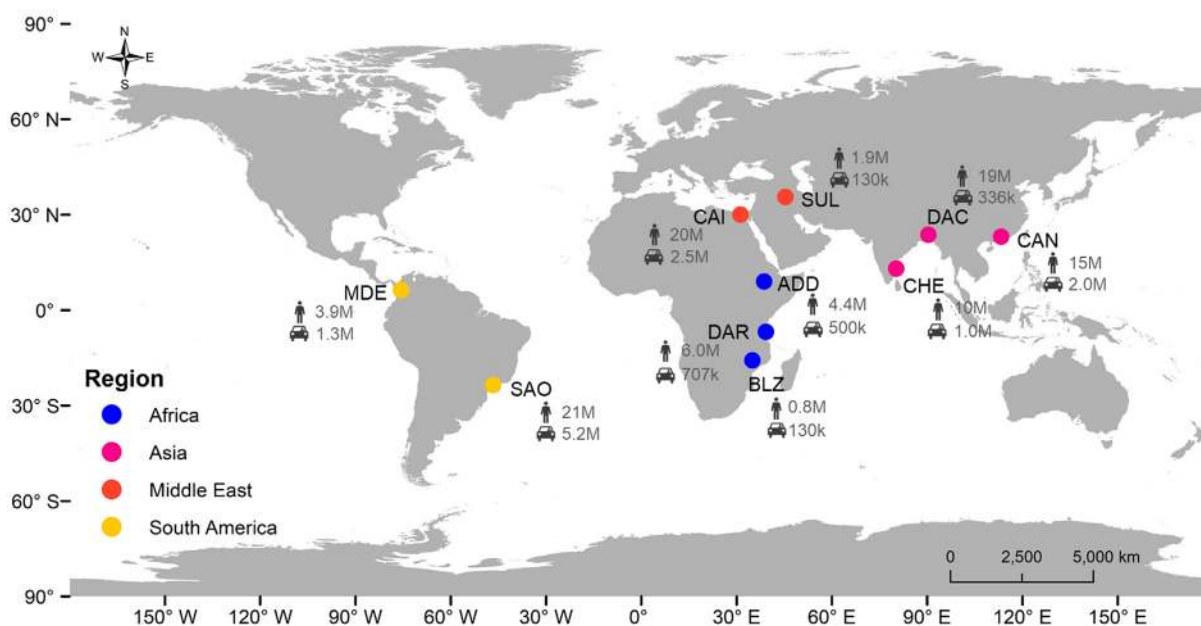

Fig. 1. Map showing location, population and number of cars in the ten studied cities: Dhaka (DAC), Chennai (CHE), Guangzhou (CAN), Medellín (MDE), São Paulo (SAO), Cairo (CAI), Sulaymaniyah (SUL), Addis Ababa (ADD), Blantyre (BLZ), and Dar-es-Salaam (DAR).

PM$_{2.5}$. We additionally calculated the 75th percentile (P75) and repeated the analysis already described above to differentiate the trends of fan-on and recirculation settings.

In-car concentrations generally varied across cities, depending on local air pollution levels, which is a function of traffic and environmental and geographical features in each city. Thus, adopting an approach that enabled an understanding of the relative variation across cities, rather than the absolute magnitude of the concentrations, was important. We normalised one-minute average PM$_{2.5}$ concentration data (C_{norm}), shown by Eq. (1) (Shaker, 2018), to 'unity-based normalisation' – also referred to as 'feature scaling' – which brings all values to between 0 and 100 (indicating to the worst and the best in-car exposure conditions).

$$Cnorm = \frac{Cx - Cmin}{Cmax - Cmin} \times 100 \qquad (1)$$

where C_x is the instant concentration at each minute, C_{max} and C_{min} are the highest and lowest observed PM$_{2.5}$ concentrations for the whole dataset. Furthermore, we calculated the arithmetic mean of the normalised data by periods of the day under each setting, to estimate an overall mean ($\sum C_{norm}$; Eq. (2)) for each city. Like C_{norm}, $\sum C_{norm}$ can range between 0 and 100, with values closer to 0 showing the best setting (an ensemble of all period) in-car exposure conditions.

$$\Sigma Cnorm(setting) = \frac{C_{norm}(MP) + C_{norm}(OP) + C_{norm}(EP)}{3} \qquad (2)$$

Finally, we estimated $\sum C_{norm}$ (overall), which also ranges between 0 and 100 and provides an overall mean for each city (an ensemble of all settings and period by city).

$$\Sigma Cnorm(overall) = \frac{\Sigma C_{norm}\,(fan-on) + \Sigma C_{norm}\,(rec) + \Sigma C_{norm}\,(open)}{3} \qquad (3)$$

The inhaled doses of PM by car commuters depend on the respiratory rate (which varies according to individual characteristics such as gender, age and physical conditions of commuters), the concentration of PM$_{2.5}$ inside the cabin and the time spent to complete a trip. The car commuters PM$_{2.5}$ inhaled dose was estimated using Eq. (4), adapted from the US Environmental Protection Agency (1992):

$$D_{pot}\left[\mu g\ kg^{-1}\ h^{-1}\right] = \frac{C_a \times IR}{BW} \qquad (4)$$

where C_a is the pollutant concentration ($\mu g\ m^{-3}$), IR is the inhalation ratio ($m^3\ h^{-1}$), which was described for adult males while seated as $0.8184\ m^3\ h^{-1}$ (Hinds, 1999), and BW is body weight (in kg) for individuals, taken as 75.4 kg. The inhaled dose per kilometer travelled is also represented to eliminate the differences in route length and the time spent inside cars among the ten cities to allow a relative comparison (Eq. (5)).

$$Inhaled\ dose\ [\mu g/km] = \frac{C_a \times IR \times t}{distance\ traveled\ (km)} \qquad (5)$$

where t is the time of each trip (h) and the distance travelled represents the length of the route in each city.

2.5. Quality assurance

All instruments were purchased approximately one month before the experimental work and were hence already calibrated by the manufacturer. Previous studies have revealed that the performance of the Dylos has been validated in comparison with multiple conventional gravimetric PM$_{2.5}$ and PM$_{10}$ monitors in urban areas (Carvlin et al., 2017; Han et al., 2017; Holstius et al., 2014; Jiao et al., 2016; Kumar et al., 2017; Lim et al., 2018; Manikonda et al., 2016; Northcross et al.,

2013; Semple et al., 2015; Steinle et al., 2015; Yuchi et al., 2019) and the agreement has been consistently high (Table S6). In addition, we carried out five days of co-located measurements with a high-end optical particle spectrometer (GRIMM model 11-C), as shown in Figs. S2–S3. The data was recorded in 1-minute intervals and a 10-minute average was calculated to compare the concentration values. High agreement was found among all Dylos monitors used in the study as the Pearson correlation coefficient (r) ranged from 0.78 to 0.99 and 0.92–0.99 for PM$_{10}$ and PM$_{2.5}$, respectively (Figs. S4–S5). A reasonable correlation was found between the Dylos and the reference monitor (Grimm), with r ranging from 0.65 to 0.88 and 0.82–0.91, for PM$_{10}$ and PM$_{2.5}$, respectively (Fig. S6). Dylos is an affordable equipment and therefore the accuracy of the data generated is limited. Nevertheless, the dataset is an innovative strategy to provide the first insights on the main determinants of pollution in traffic environments.

3. Results and discussion

3.1. Overall differences in PM concentrations

Fig. 2a and b shows the overall average concentrations of in-car PM$_{2.5}$ and PM$_{10}$ over the entire sampling duration in each city. PM concentrations varied greatly across the 10 studied cities, reflecting regional consistencies of in-car exposure. African (ADD, BLZ, DAR) and Asian cities (DAC, CHE, CAN) showed relatively higher average concentrations with wide variation ranges when compared with Latin-American and Middle-Eastern cities. For example, the average concentration of PM$_{2.5}$ (65 $\mu g\ m^{-3}$) and PM$_{10}$ (76 $\mu g\ m^{-3}$) in DAR was the highest among the cities as opposed to much lower average PM$_{2.5}$ (PM$_{10}$) concentrations in SAO and MDE of 16 (28) $\mu g\ m^{-3}$ and 18 (36) $\mu g\ m^{-3}$, respectively (Fig. 2). Dominant sources of PM$_{2.5}$ and PM$_{10}$ pollution (Table S4) in each city vary, including vehicular emissions, dust resuspension from unpaved roads, biomass burning and industrial and urban activities. These sources can qualitatively explain the underlying factors that may have caused observed variations in PM concentrations.

Table S7 summarises the detailed statistics for in-car PM$_{2.5}$ and PM$_{10}$ concentrations ($\mu g\ m^{-3}$) under each setting during three times of the day. The corresponding boxplots for PM$_{2.5}$ and PM$_{10}$ for all ten cities are shown in Figs. 3 and S7, respectively. Windows-open resulted in the highest average concentrations of PM$_{2.5}$(PM$_{10}$) during MP: ADD [136(364)], followed by BLZ [97(223)], DAR [106(357)], CHE [74 (165)], DAC [65(156)], CAN [108(184)], and CAI [86(224)]. Relatively lower levels of PM$_{2.5}$(PM$_{10}$) were observed in MDE [37(77)], SAO [39 (66)] and SUL [32(–)] $\mu g\ m^{-3}$. The fan-on setting resulted in lower PM levels than windows-open, while recirculation resulted in the lowest concentrations by preventing ambient air pollution from entering the car cabin. For windows-open, mean concentrations of PM$_{2.5}$ across cities during MP ranged between 32 (SUL) and 136 (ADD) $\mu g\ m^{-3}$, while the corresponding mean PM$_{10}$ concentrations ranged from 66 (SAO) to 364 (ADD) $\mu g\ m^{-3}$. For fan-on, mean PM$_{2.5}$ concentrations during MP were lowest in SUL (25 $\mu g\ m^{-3}$) and highest in DAR (85 $\mu g\ m^{-3}$), while the corresponding mean PM$_{10}$ concentrations ranged from 54 (SAO) to 164 (DAR) $\mu g\ m^{-3}$. For recirculation, the lowest mean PM$_{2.5}$ concentrations during MP were in SUL (6 $\mu g\ m^{-3}$) and highest in DAR (80 $\mu g\ m^{-3}$), while the corresponding mean PM$_{10}$ concentrations ranged from 11 (SAO) to 152 (DAR) $\mu g\ m^{-3}$. This preliminary analysis reflects how car commuters in these cities are exposed to varying PM levels, depending on both car settings (windows-open > fan-on > recirculation) and period of the day. Compared with other settings, windows-open consistently showed higher levels of both PM$_{2.5}$ and PM$_{10}$ throughout the whole study, regardless of city and period of the day, due to the car cabin's direct exposure to the external environment.

Further analysis was undertaken to investigate correlations between city-specific economic developments and in-car exposure to PM$_{2.5}$, which is a proxy for traffic emissions and on-road ambient conditions.
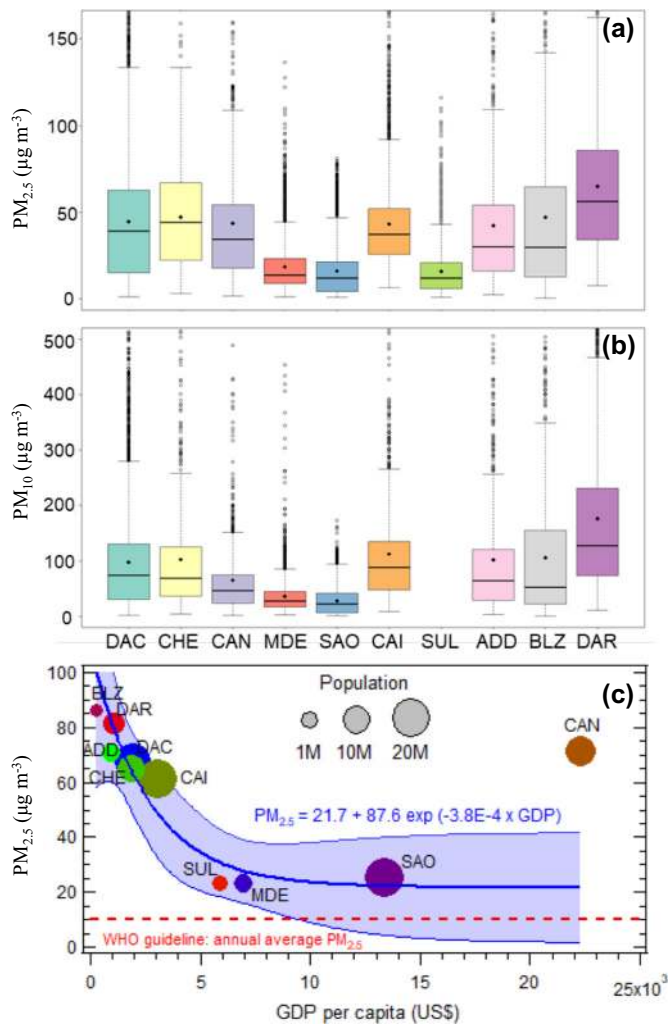
Fig. 2. Boxplot of (a) $PM_{2.5}$ and (b) PM_{10} concentrations ($\mu g\ m^{-3}$) measured during all settings and times of the day for the ten cities as denoted by city code. The top, middle, and bottom line of the box represents the 75th, median, and 25th percentiles, respectively. The diamond shape point represents the arithmetic mean. Error bars outside the box represent 1.5-times the interquartile range and outliers are depicted as open circles. (c) Car exposure to the arithmetic mean of $PM_{2.5}$ concentrations in windows-open setting, representing ambient on-road concentrations, against the city-specific gross domestic product per capita (GDP, in US$) for the year 2019 (see references in Table S8). The solid blue line shows the exponential fit to the observed data along with associated 80% confidence interval (blue bands). The circle size represents the population in each city. The smallest (BLZ) and largest (SAO) size of bubbles represent a population of 0.8M and 21M, respectively.

Fig. 2c shows a negative correlation between average $PM_{2.5}$ exposure under windows-open conditions and per capita GDP for each city. An exponential decay in $PM_{2.5}$ exposure with increasing GDP highlights a social inequality where cities of lower GDP growth rate, mainly in Asian and African countries, show higher $PM_{2.5}$ exposure for in-car users and vice-versa (Fig. 2c). CAN is an outlier with the highest GDP and high in-car $PM_{2.5}$ exposure, which may be explained by a compromised focus on environmental problems brought by rapid development, as is the case for major cities in developing countries like China (Han et al., 2019; Lelieveld et al., 2015; Zhang et al., 2010), where impressive economic growth (~7% per year, Gdstats, 2017) occurs at the cost of increased pollution exposure. These correlations (Fig. 2c) are among the first of such observations, which illustrate that the chosen cities have both the similarities and the discrepancies. Previous studies have shown a similar correlation between outdoor $PM_{2.5}$ concentration and the city-specific (Anenberg et al., 2019) or country-specific GDP

(Hasenkopf et al., 2016). The trend exhibited by CAN, as an outlier, has also been observed in other Asia-Pacific countries (Hasenkopf et al., 2016) where environmental protection efforts have not kept up with the staggering rates of economic advancement within these progressive countries. The rare economic development of CAN far outpaced the GDP of other Chinese cities. For example, the GDP of CAN was 4.3 billion in 1978 that increased by 558-times to 2.4 trillion in 2019; compared with 10.9 billion and 27.3 billion for Beijing and Shanghai in 1978 increasing by 321 and 293-times to 3.5 trillion and 8 trillion in 2019, respectively (TCYB, 2020). Obtaining the in-car concentrations under similar experimental conditions (i.e. during different times of the day and the same car settings) are not feasible for other cities and are therefore not considered in the current analysis. However, expanding a similar analysis to other cities, including those in China, would broaden the perspective and understand similarities and the discrepancies among on-road exposure concentrations with the city-specific economic development.

3.2. Effect of car settings on in-car exposure

3.2.1. Ventilation settings

PM concentrations under the recirculation setting were found to be the lowest across all cities (Section 3.1). This setting may reflect in-car background PM levels, given that it represented sealed cabin conditions. Hence, the subtraction of recirculation setting concentrations from fan-on and windows-open concentrations should provide an estimate of increased in-car PM concentrations caused by ingress of outdoor pollutants from different pollution sources in each city. Fig. 4 shows concentration differences between windows-open recirculation modes for coarse ($PM_{2.5-10}$) and fine ($PM_{2.5}$) particles, which are a proxy for non-exhaust sources (i.e., road dust resuspension, road-tyre wear) and exhaust emissions, respectively. In-car exposure to coarse particles was found to increase from 195% (MDE) to 1450% (BLZ) during windows-open when compared with recirculation. A lower increase, from 29% (CAI and ADD) to 390% (SAO), was observed for coarse particles during fan-on when compared with recirculation. Corresponding increases in fine particle concentrations were also higher for windows-open modes, ranging from 81% (DAR) up to 668% (BLZ) as opposed to 21% (CAN) to 385% (SAO) during fan-on when referenced against recirculation. Although the recirculation mode showed the lowest concentrations, it should be used intermittently to avoid pollution hotspots (Section 3.4) as well as accumulation of exhaled carbon dioxide by car occupants (Jung et al., 2017). While the experiments were unified as much as possible across the cities by using, for example, the same car in each city and similar occupancy, routes and car settings, the very same car was not used in all cities and thus the difference in the type and age of the vehicles used (Table S2) could have influenced the cabin filter efficiency. Despite this, irrespective of the city and type of car used, this trend indicates that car cabin filters are generally more effective in removing coarse particles when compared to fine particles. A similar trend was noted in previous studies that carried out in-car measurements in Guilford (Kumar et al., 2018a, 2018b; Kumar and Goel, 2016) and London, UK (Rivas et al., 2017). These findings also suggest that new cars should be fitted with more efficient filters, to filter fine particles along with coarse particles and reduce the overall exposure of car commuters to high $PM_{2.5}$ and PM_{10} levels.

3.2.2. Periods of the day

During windows-open, mean $PM_{2.5}$ concentrations during EP were generally lower than during MP, ranging between 7% (CHE) and 63% (ADD) (Table S7). This observation does not hold for all cities; for example, $PM_{2.5}$ concentrations during EP in DAC and BLZ were 3% and 12% higher than MP. However, windows-open during OP predominantly resulted in between 16% (DAC) and 73% (ADD) lower $PM_{2.5}$ concentrations when compared with MP under the same setting. Similarly, mean $PM_{2.5}$
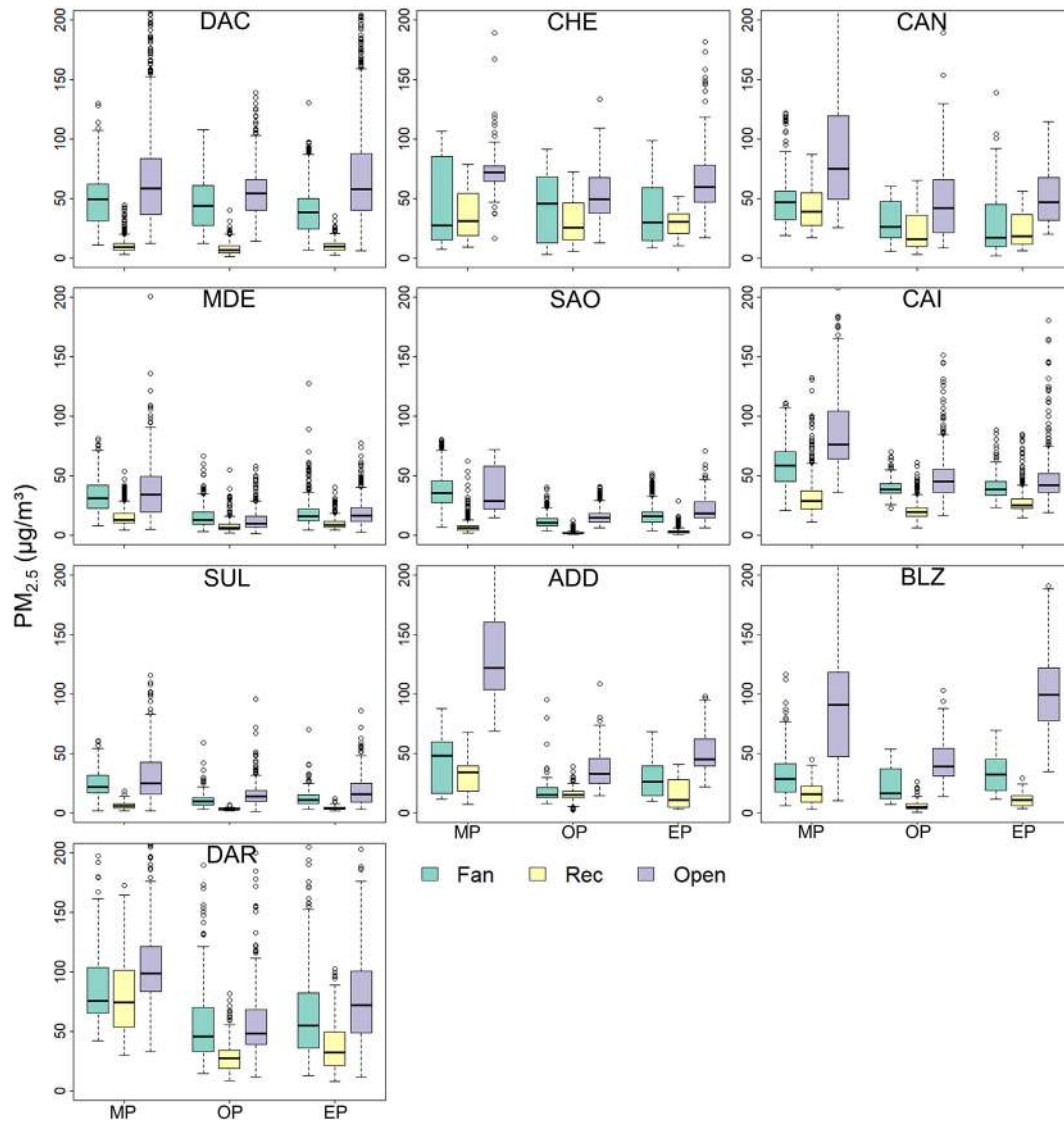
Fig. 3. Boxplot of PM$_{2.5}$ levels for ten cities as denoted by city code. The top, middle, and bottom of the box represent the 75th, median, and 25th percentiles, respectively. Error bars outside the box represent 1.5-times the interquartile range and outliers are depicted by open circles.

concentrations during OP were between 10% (CAN) and 60% (BLZ) lower than during EP for windows-open (Table S7). However, mean PM$_{2.5}$ concentrations for CAI under windows-open during OP were 4% higher than during EP. To assess the variations in PM concentrations, we estimated relative standard deviation (RSD) for each city/setting. RSD indicates whether or not the 'regular' standard deviation is a small or a large quantity when compared to the mean of the data set. As expected, the RSD ranged substantially for the three settings: from 29.5% (CHE) to 96.7% (CAN) during windows-open, from 19.1% (CAI) to 91.8% (CAN) during fan-on, and from 37.8% (CHE) to 94.6% (SAO) during recirculation (Section 3.5). This indicated that there are numerous determinants of in-car concentrations, including period of the day, proximity to traffic emissions, road conditions, urban layout, efficiency of the vehicle filter, and ambient weather conditions.

A comparison of in-car concentrations from different time periods revealed that PM$_{2.5}$ concentrations were higher during MP than OP for major cities under all three settings (MP/OP>1; Fig. 5). During EP hours, major cities also showed PM$_{2.5}$ concentrations higher than OP, although EP/OP ratios were lower than MP/OP. While the MP/OP ratio ranged from 1.1 (DAC and CHE) to 3.7 (ADD), EP/OP ranged from 0.9 (ADD, CHE and CAN) to 2.5 (BLZ). Cities that conform with the MP/OP > EP/OP pattern (all cities except DAC, CHE and BLZ) indicate that car

commuters are exposed to higher PM$_{2.5}$ concentrations during MP hours than at any other period (Section 3.1). Conversely, there are cities (DAC and CHE) where travelling during peak or off-peak hours did not influence concentrations; i.e. where MP/OP and EP/OP ratios were ~1 (Fig. 5). Cluster analysis based on these patterns clearly showed two groups of cities (Pearson $r > 0.7$), aggregating CHE, CAN, CAI, MDE, ADD, SAO and SUL in one group, and DAC, BLZ and DAR in another group (Fig. S8). In order to test the correlations between the ambient PM$_{2.5}$ concentrations and measured in-car PM$_{2.5}$ concentrations during windows-open, we compared these data for the same days and periods of our measurements in cities where such data were available (Fig. S9). As expected, poor correlations were found ($R^2 \leq 0.5$). This is because the in-car concentrations during windows-open are representative of on-road concentrations while ambient urban concentrations are typically measured by monitoring stations that are usually installed away from the roadside and/or in relatively quieter places and at different heights (generally higher than the exposure height of sitting occupants in cars). Therefore, ambient urban concentrations will not capture peak concentrations encountered by the on-road measurements, owing to their close proximity to the exhaust of on-road vehicles and traffic congestion and the built-up environment surrounding the roads.
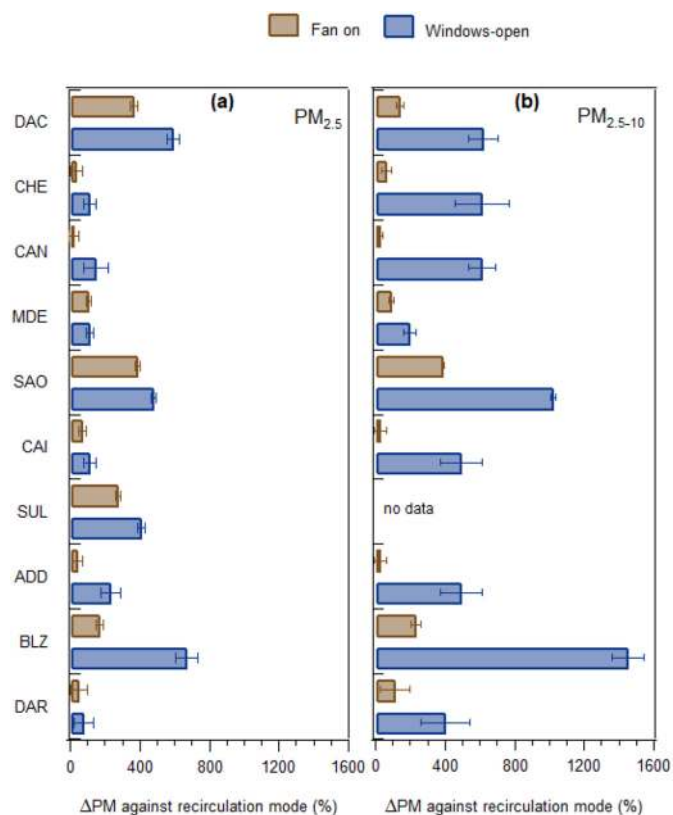
Fig. 4. Change in-car concentrations during fan-on and windows-open settings against recirculation mode for (a) fine ($PM_{2.5}$) and (b) coarse ($PM_{2.5-10}$) particles across all cities.

3.3. Ratios of in-car $PM_{2.5}/PM_{10}$

Fig. 6 shows the fractional contributions of fine particles to the total PM. Under fan-on, PM concentrations were typically dominated by the fine fraction ($PM_{2.5}/PM_{10} > 0.5$) for most cities (except for CAI and DAR) during all periods of the day despite the use of different car models and ages. Under recirculation, the same pattern was observed for most cities (except for DAC). These patterns may be attributed to low filter effectiveness in removing fine particles when compared to coarse particles (Section 3.2.1). To normalise the effect of different car filters, we focus on windows-open setting where cities like CHE, MDE and SAO showed this ratio to be higher than 0.5 during MP. In other cities (DAC, CAI, ADD, BLZ and DAR), these ratios showed values lower than 0.5, highlighting the contribution of coarse particles from soil and dust resuspension near roads. Higher ratios were observed during MP (Sections 3.1 and 3.2.2), which may be attributed to lower resuspension of coarse particles in early morning hours due to road pavement wetness caused by overnight dew, as also reported by previous studies (Kumar and Goel, 2016; Kumar et al., 2017). The high contribution of coarse particles to PM concentrations may be a result of other sources, such as the impact of the Savanna climate in DAR (measurements in DAR were taken between August and September, the driest months of the year in this region; Sections S1-S2) and the desert Saharan dust in CAI (Querol et al., 2019). A recent study in Cairo (Abbass et al., 2020) also showed high coarse particle fractions. In CAN, the $PM_{2.5}/PM_{10}$ ratio was >0.5 for all periods of the day, reaching 0.9 in some instances, showing a dominance of fine particles. These observations coincide with the challenges of high fine particles from both primary and secondary aerosol formation from inorganic (sulfate and nitrate compounds) and volatile organic compounds (Marlier et al., 2016) that several Chinese cities are facing, due to rapid industrial and economic advancements (Zhao et al., 2019). The above observations also suggest that the mixture of particles that car commuters are exposed
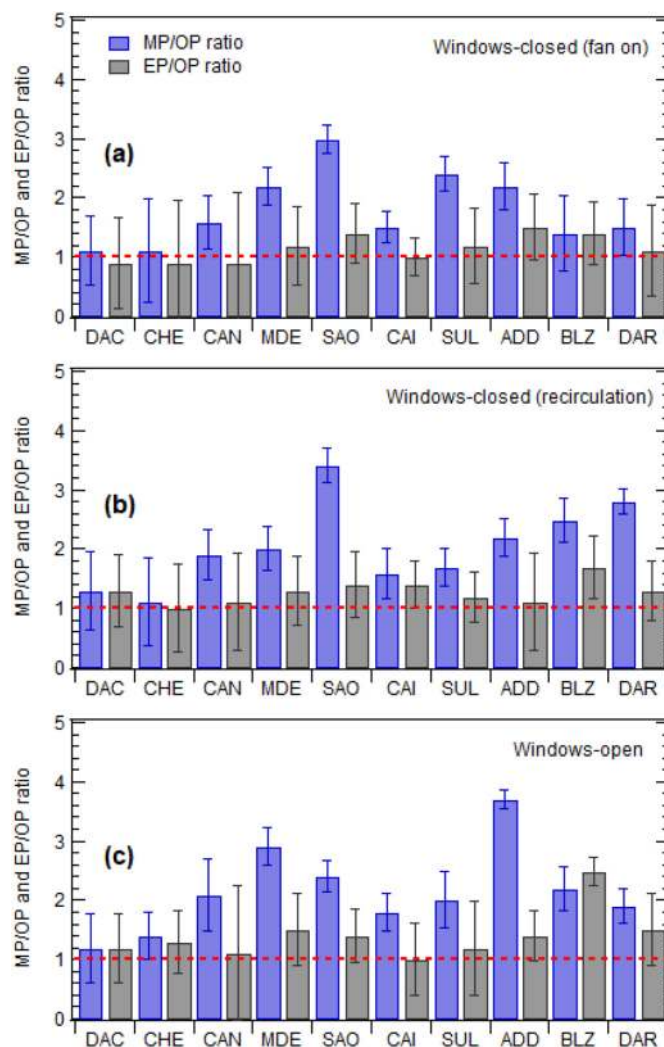

Fig. 5. Morning peak/off-peak ratio (MP/OP) and evening peak/off-peak ratio (EP/OP) for $PM_{2.5}$ in-car concentrations during fan-on, recirculation and windows-open settings across the ten cities. Error bars represent the standard deviation of the average value obtained in each city. Red dashed line represents a ratio of 1.0.

to predominantly constitute the fine fraction ($PM_{2.5}/PM_{10} > 0.5$), especially during fan-on and recirculation settings. These findings reinforce earlier observations (Section 3.2.1) that cars, despite their different models and ages, are generally more efficient in removing the coarse fraction of particles than their finer counterparts. The lower ratio (<0.5) of $PM_{2.5}/PM_{10}$ during windows-open represents on-road ambient concentrations (Section 3.1) and highlights the significance of local sources of coarse particles, as observed in developing cities such as Delhi (Hama et al., 2020), Cairo (Abbass et al., 2020) and São Paulo (Nogueira et al., 2020), where resuspension of dust from road surfaces and nearby bare lands is quite common.

3.4. Intracity spatial variation of $PM_{2.5}$ within individual routes

Spatial variation in PM concentrations highlights congested and most polluted sections of a route. Hereafter, route segments with local data points indicating average $PM_{2.5}$ higher than P90 (defined in Section 2.4) are referred to as hotspots (Goel and Kumar, 2014). Concentration values, equivalent to P90, varied under individual settings in each city (Table S9). Fig. 7 shows $PM_{2.5}$ hotspots during windows-open in which percentages of the route lengths, indicated by in red, are evident for most cities. The corresponding maps for the other two
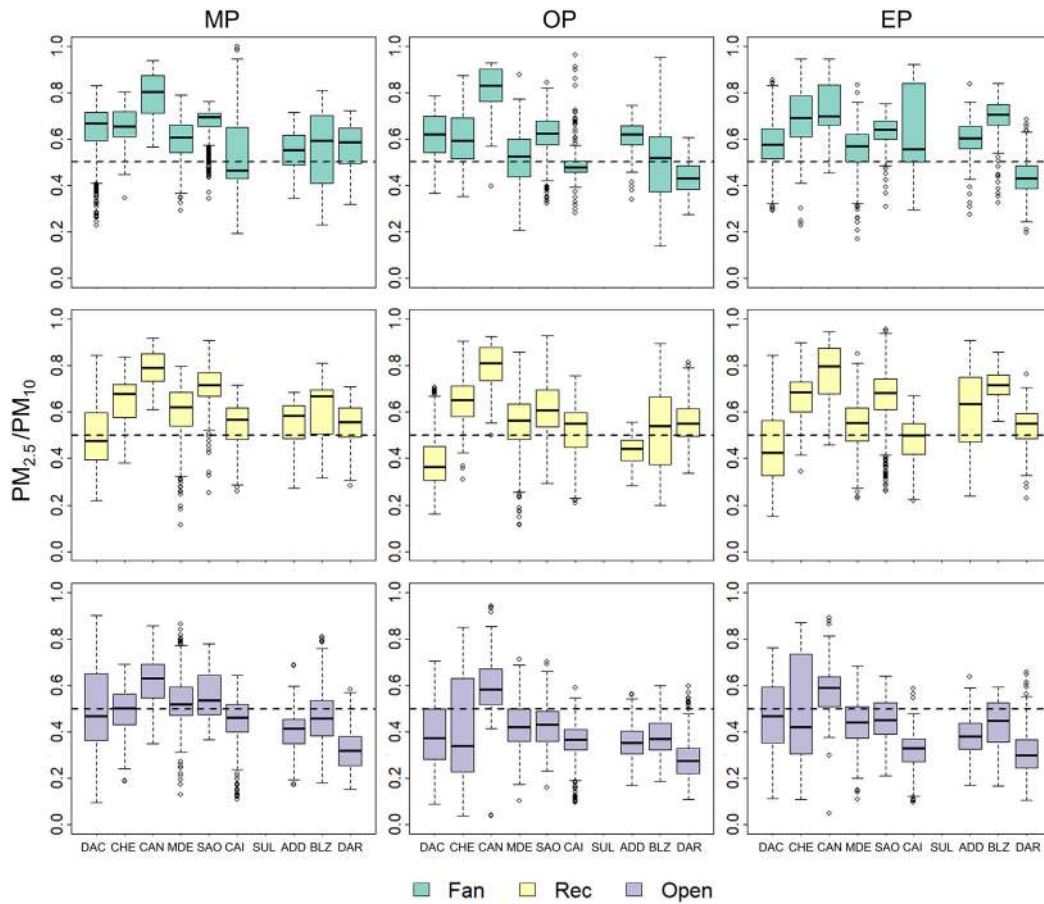
Fig. 6. Boxplot of the $PM_{2.5}/PM_{10}$ ratio for all cities at different periods of the day and ventilation settings. The top, middle, and bottom of the box represent the 75th, median, and 25th percentiles, respectively. Error bars outside the box represent 1.5-times the interquartile range and outliers are depicted by open circles. The dashed line indicates $PM_{2.5}/PM_{10}$ of 0.5.

settings are shown in Figs. S10–S12 and the percentages of the route-length in Table S9.

During windows-open, $PM_{2.5}$ hotspots covered up to about one-third of the total route length (Table S9). For example, CAN had the greatest route-length (32%) identified as hotspot, followed by DAR (23%), CHE (17%), DAC (14%), SUL (12%), CAI (9%), BLZ (7%), MDE (4%), ADD (3%), and SAO (0%), where no hotspots were identified. Detailed inspection of the data showed that these hotspots were concentrated along the S296 Rd. and Xinhua Express in CAN and along Uhuru St. and Changombe Rd. in DAR (Fig. 7), mainly due to high traffic congestion as observed by field researchers. CHE was next in line for hotspots, occurring at Tharamani Rd. and Velachery Main Rd. (Fig. 7), both of which are commercial streets and are hence, typically, highly used. CAI followed, with hotspots concentrated at the intersection of El-Orouba and El-Nozha Av., where a bridge was under construction during data collection, resulting in traffic congestion (Abbass et al., 2020). MDE had only a modest route-length (4%) of hotspots, observed at the intersection of South Highway and 30th St., locally considered to be a congested bottleneck (Fig. 7). SAO showed no hotspots, whereas a notable decline in $PM_{2.5}$ concentrations was observed at the southern section of the route near Ibirapuera Park, a 158 ha green area, during fan-on and windows-open (Figs. 7 and S11). A similar trend was observed at this part of the route by Brand et al. (2019) during cycling measurements in SAO. This suggests that the percentage of hotspots is also dependent on urban layout and route characteristics, and that green areas along a route may result in a decline in $PM_{2.5}$ concentrations. Moreover, roadside building configurations can directly affect the airflow in a city and consequently the dispersion of air pollutants within a car cabin (Zhang and Gu, 2013). Thus, a city with less overall transport emissions may show higher on-road PM concentrations if

congested traffic conditions persist and the airflow is restricted by building layouts (Kumar et al., 2015a, 2015b, 2016). This is evident in the African city of ADD, for example, where P90 is 181% higher than those in SAO, despite the number of on-road vehicles in ADD being less than one-fifth of the car count in SAO (Table S3).

During fan-on and recirculation, hotspots were nearly zero across all cities (Table S9). This was mainly due to the fact that the same concentration scale was used for all three settings and that $PM_{2.5}$ concentrations were significantly higher for windows-open when compared with the other two settings (Figs. S10–S12).

Similar to P90, we also estimated P75 (Table S9), showing that some cities may encounter high peaks (exceeding P90) of $PM_{2.5}$ concentrations during small percentages of route-lengths but exceed P75 for large percentages of route-lengths. For example, SAO has nearly no P90 exceedances but 86% of its route-length exceeded P75 (Table S9). Likewise, 32% of the route-length in CAN exceeded P90 while more than two-thirds of the total route-length (65%) exceeded P75. We extended the analyses to carry out hierarchical cluster analysis based on spatial variations in concentrations (Fig. S13), to understand similarities between cities and classify them into groups based on P75/P90 and on the percentage of route-length exceedances (Table S9). Cluster analysis showed three main groups (Fig. S13). The first group (SAO, MDE and SUL) had the lowest P90 under all three settings, indicating lower background concentrations (Fig. 4). The second group (ADD, BLZ and DAR) showed the highest P90 and P75 under all settings and the lowest average car speed (16 km h^{-1}; Fig. S14), indicating heavy traffic congestion. The third group (DAC, CAI, CAN and CHE) presented the highest percentages of route-lengths exceeding P90 under windows-open (Table S9), as well as the lowest amount of congestion, which was indicated by comparatively high mean car speeds (24 km h^{-1}; Fig. S14).
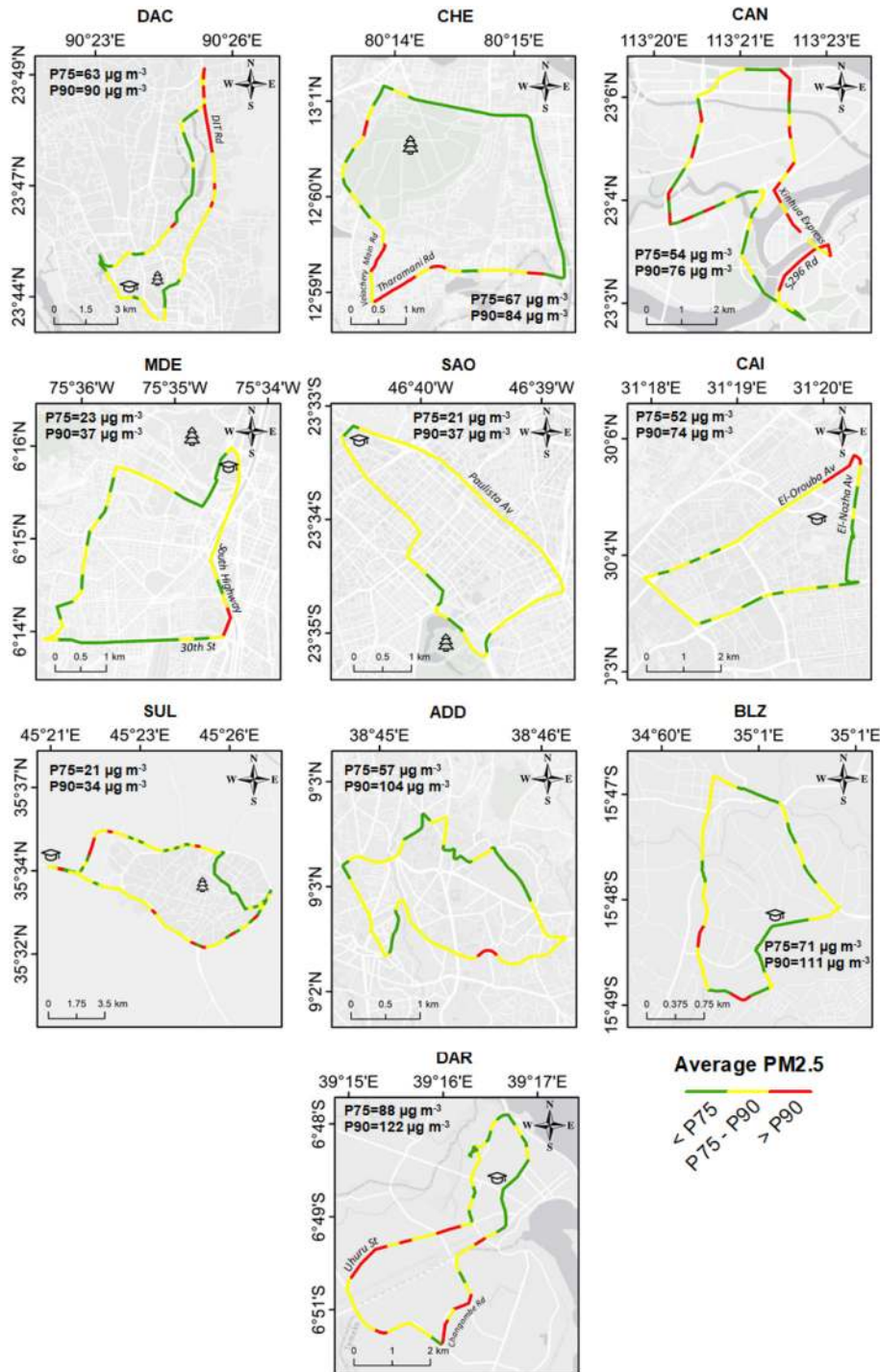
Fig. 7. Spatial variation of average PM$_{2.5}$ concentration (µg/m^3) across the route in each city in all periods of the day during windows-open setting. The averages were calculated in every ~300 m with all the GPS data (latitude and longitude) available (Table S9). The concentration scale varies according to the P75 and P90 calculated of each city (Table S9). The academic cap symbol indicates the location of the University and the tree symbol indicates the presence of a Park.

The above spatial analysis highlighted the specific geographical features of route sections that are considered pollution hotspots. It may also allow car commuters to avoid hotspots during trips by choosing alternative route sections or turning on the recirculation to decrease in-car exposure. Previous work has reported that time spent at hotspots around traffic intersections can represent as little as 2% of total commuting time and yet account for up to one-fourth of total exposure doses (Goel and Kumar, 2015). The above observations reinforce these findings (i.e. avoid hotspots to reduce overall inhaled doses; Section 3.6) across cities and illustrate that cities with the highest concentrations,

exceeding P90/P75, do not necessarily show the highest percentage of the route-length with P90/P75 (Table S9).

3.5. Global comparison of exposure concentration across cities

We normalised concentration values within a range of 0 to 100 in order to bring all values to the same scale and allow for a global comparison between different cities (Table S11). Since the normalised concentrations (C_{norm}) are derived from absolute concentrations (Section 2.4), there is a strong correlation ($r^2 > 0.99$) between them (Fig. 8a). ΣC_{norm}
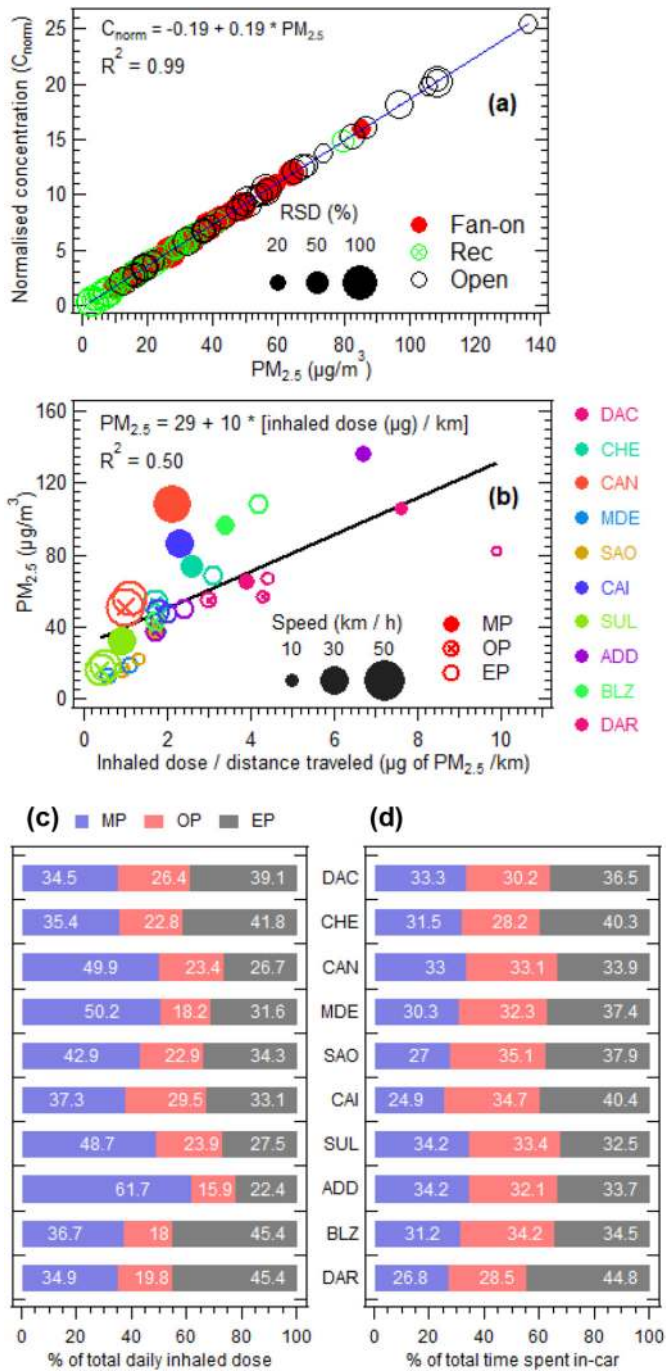
Fig. 8. (a) Normalised and absolute concentrations of PM$_{2.5}$ at the ten studied cities for the three settings. The circle size represents the Relative Standard Deviation (RSD; %) in each city and each period and setting. The smallest (CAI, fan-on, OP) and largest (CAN, windows-open, OP) size of bubbles represent an RSD of 19.1% and 96.7%, respectively. (b) Estimated inhaled doses of PM$_{2.5}$ per kilometer travelled against in-car PM$_{2.5}$ concentration under windows-open setting during MP, OP and EP periods across the ten cities. The circle size represents the average car speed in each city during different periods of the day. The circles are colour-coded to indicate each city. The relative contribution during MP, OP and EP hours to the total daily (sum of three periods) inhaled dose of PM$_{2.5}$ during windows-open setting across the ten cities, showing percentages of (c) total inhaled doses, and (d) total time spent inside the car.

was estimated (Table 2) for each city as an arithmetic means of the C_{norm} for different settings (Section 2.4). Both followed the same trend (Section S4) as for concentrations (i.e. windows-open>fan-on>recirculation) and time of day (MP > EP > OP; Section S4).

We grouped the cities based on the linkage (Euclidean) distances using cluster analysis (Fig. S15). This allowed us to classify cities into

Table 2
Global normalisation values (global ΣCnorm) of PM$_{2.5}$ at the ten studied cities for the three-day periods (MP, OP and EP) and the overall ΣCnorm by city. The cell colour uses the scale from green to red and the conditional formatting uses the P75 values as the midpoint in excel function.

City	ΣCnorm (open)	ΣCnorm (fan-on)	ΣCnorm (rec)	ΣCnorm (overall)
DAC	12	8.1	1.6	7.2
CHE	12.2	7.8	5.7	8.6
CAN	13.1	6.2	5.1	8.1
MDE	4.1	4	1.9	3.3
SAO	4.4	3.7	0.6	2.9
CAI	10.7	8.7	5	8.1
SUL	4.1	3	0.6	2.6
ADD	13.3	5.7	3.8	7.6
BLZ	16.2	5.6	1.9	7.9
DAR	15.1	12.7	8.3	12.0

PM concentration-based categories in accordance with their proximity to each other. Fig. S16 shows a map of all 10 cities classified into three groups, represented by low, intermediate and high levels of PM exposure for car commuters. The first group consists of cities with low PM concentration (Figs. S17–S20), including both Latin American cities (MED and SAO) and a Middle-Eastern city (SUL) that had C_{norm} values <P75 during three periods of the day and settings. The second group included cities with intermediate PM concentrations, taken as >P75 in more than one period and setting. This group included three Asian cities (CAN, CHE and DAC), one Middle-Eastern city (CAI) and two African cities (ADD and BLZ). Finally, the third group included cities with high PM concentrations that had C_{norm} values >P90 for all settings. Only DAR fell into this group.

The overall ΣC_{norm} (Table 2), which represents an ensemble of exposure conditions for each city, followed the categorisation based on cluster analysis above. For example, its values were the best (lowest) for the first group of cities (3.3, 2.9 and 2.6 for MED, SAO and SUL, respectively) and the worst (highest) by nearly four times in the third group (12 for DAR). The rest of the cities fell into the intermediate group, where ΣC$_{norm}$ ranged from 7.2 to 8.6 (Table 2).

Even the setting-specific C_{norm} for all three settings was consistently the lowest in the first group (Table 2), confirming the best exposure conditions when compared with other cities. As expected, exposure conditions were the worst under windows-open for most cities (except for the first group), with C_{norm} values ranging from 10.7 (CAI) to 16.2 (BLZ). Four out of 10 cities under windows-open present the worst (>P90) exposure conditions and another three intermediate (>P75) exposure conditions. Under fan-on and recirculation, C_{norm} fell into the intermediate exposure group for all cities except for DAR, which had a high exposure group (Table 2).

The above analysis enabled the classification of studied cities into groups, to explore similarities between cities in the same group and learn from the strategies adopted by cities in the less polluted groups. For example, the first group (MED, SAO and SUL) was clearly the best

exposure group, where exposure conditions under all three settings remained low (i.e., <P75). In SAO, the Program for the Control of Air Pollution Emissions by Motor Vehicles (PROCONVE) has effectively reduced vehicular emissions nationwide by limiting air pollution violations in Brazilian cities (Andrade et al., 2017). In MED, the Integrated Plan for Air Quality Management (PIGECA), adopted in 2018, introduced monitoring and control strategies for mobile sources, including increased controls such as on-road emissions testing and circulation restrictions for vehicles during periods of high $PM_{2.5}$ concentrations (AMVA, 2017). This strategy has effectively helped the local air quality index to be recategorised from Unhealthy to Moderate (AMVA, 2019). In SUL, no air pollution control measures have been implemented, but recent actions to improve fuel quality, phase out old cars and upgrade vehicle standards, along with a comparatively small population of road vehicles (Table S3) and therefore traffic congestion (Fig. S14), appears to have improved in-car exposure (MOP, 2019). The classification for the rest of the cities could change between low and intermediate exposure groups, depending on whether a specific setting is considered or an overall average of the three settings (Table 2). Nevertheless, windows-open resulted in up to a four-fold deterioration in exposure conditions in the seven cities of the second and third groups.

3.6. Relative exposure doses

The inhaled doses for $PM_{2.5}$ were plotted against in-car $PM_{2.5}$ concentrations and the corresponding car speeds are represented by the size of circles (Fig. 8b). We focus on a windows-open setting to eliminate the effect of cabin filter efficiency that varies between different cars and allow a fair comparison between different cities by minimising the uncertainties caused by different types of car and their cabin filters. We also discuss inhaled doses per unit time and body weight ($\mu g \ kg^{-1} h^{-1}$) and distance driven ($\mu g \ km^{-1}$) to make observations about traffic congestion in cities and its implications for the dose inhaled by car-users while eliminating the variations introduced by differences in car models used (Table S12). Generally, a linear correlation is noted between doses and concentrations (Fig. S21). The following discussion is based on $\mu g \ km^{-1}$, which allows a fair comparison by estimating the potential dose inhaled by the car commuter to cover the same distance, and thereby taking into account factors that may impact the time spent inside a car due to discrepancies in the traffic conditions and route length among the ten cities. For example, the lowest $PM_{2.5}$ inhaled dose (0.4 $\mu g \ km^{-1}$) was estimated for SUL during OP, while the highest (9.9 $\mu g \ km^{-1}$) for DAR during EP. SUL belongs to the first group of cities, where car commuters are exposed to low PM concentration, while DAR is the only city in the third group, with the highest exposure concentrations (Section 3.5). The mean car speed in DAR was the lowest among all cities, ranging from 6.4 (EP) to 10.7 km h^{-1} (MP), which is much lower than in SUL (second highest speeds), which ranged from 33.4 (MP) to 35.2 km h^{-1} (EP). These findings reinforce that traffic congestion (Section 3.4) can disproportionately affect PM exposure. Although the highest PM concentrations were observed in DAR during MP (1.3-times higher than EP), EP hours resulted in the highest inhaled dose, which also highlights the impact of traffic congestion where car speeds decrease by 1.6-times in EP when compared with MP. Exceptions to the linear relationship (inhaled dose versus PM concentrations) were observed for three cities (DAC, CAN, DAR), where in-car concentrations for CAN averaged 108 $\mu g \ m^{-3}$ during MP, contributing to an inhaled dose of 2.1 $\mu g \ km^{-1}$. The inhaled dose in CAN is close to MDE (1.8 $\mu g \ km^{-1}$) and SAO during MP (1.7 $\mu g \ km^{-1}$), but nearly 3.6-times lower than the highest doses observed in DAR during MP. Additionally, $PM_{2.5}$ concentrations in CAN (car speeds ~43 km h^{-1}) were up to 2.9-times concentrations in MDE and SAO, where the average car speeds were ~17 km h^{-1}. The inhaled doses ranged from 0.14 to 1.18 $\mu g \ kg^{-1} h^{-1}$ across cities. The inhaled doses in Latin American cities (MDE and SAO) and SUL were 0.14, 0.17 and 0.18 $\mu g \ kg^{-1} h^{-1}$ (during OP), respectively, which were comparable (0.16 $\mu g \ kg^{-1} h^{-1}$) to those reported for

car commuters in Londrina, Brazil (Moreira et al., 2018). These findings should draw the attention of policy-makers on the importance of investing in solutions to reduce traffic congestion as a means to reduce pollution concentrations.

The percentages of total daily inhaled dose for in-car $PM_{2.5}$ (Fig. 8c) and the corresponding percentages of the total daily in-car commuting time (Fig. 8d) vary disproportionately throughout each period of the day. The word 'total' refers to the sum of MP, OP and EP. In some cases (e.g. during MP in CAI), as little as ~25% of total daily time spent corresponded to 37% of the total daily inhaled dose. In other cases (e.g. during EP in DAR), as high as ~45% of total time spent corresponded to a similar fraction (~45%) of the total daily inhaled doses. The percentage of time spent during MP ranged across cities, from as little as one fourth to as high as one third (25–34%) of total time spent, but the corresponding doses were relatively high, ranging from one third to half (34–50%) of total inhaled doses. An opposite trend was seen during OP, where the time spent in-car was similar to MP (28–35%), but the corresponding doses were much lower (16–30%). The trend for EP was more balanced, where 32–45% of total time spent corresponded to 22–45% of total doses. Such trends are expected due to less traffic volume (Section 3.1) and more favourable dispersion conditions, due to a typically higher planetary boundary layer at midday (Quan et al., 2013). The above observations also mimic the overall trend of much higher concentrations during EP than other periods (Section 3.1), explaining the dominance of doses during EP. The above observations also highlighted the determinants for inhaled doses across cities. For example, cross-correlations between inhaled doses, in-car $PM_{2.5}$ concentration, car speed, spent inside cars, and distance travelled across all cities suggests that high concentrations during MP ($r = 0.73$; Table S13) led to increased inhaled doses despite less time spent inside a car ($r = 0.67$; Table S14), and lower concentrations ($r = 0.72$; Table S14) during OP led to decreased inhaled doses. The case of EP was mixed, with higher time spent inside the car (to increase doses; $r = 0.75$; Table S15) but slightly lower concentrations (to decrease doses; $r = 0.68$; Table S15) when compared with MP and hence the resulting doses being between the MP and OP. Car speed showed an inverse correlation with inhaled doses during all periods ($r = -0.54$ to -0.59), suggesting an overarching effect of traffic congestion on inhaled doses.

4. Conclusions and future outlook

For the first time, this study presents a global assessment of in-car exposure profiles in 10 cities across four continents: Asia; Latin America; Middle-East; and Africa. PM monitoring in all cities was carried out using a similar set of laser particle counters during morning and evening peak hours as well as off-peak hours, under three different car settings (windows-open, recirculation, and fan-on) at multiple times on a predefined route.

The key conclusions drawn from this study are as follows:

- The windows-open setting exposes car commuters to the highest concentrations of both PM fractions ($PM_{2.5}$ and PM_{10}), followed by fan-on and recirculation, which may be due to direct exposure of the car cabin to the external environment. Recirculation offered the lowest $PM_{2.5}$ and PM_{10} exposure since the ingress of external dust into the car is controlled. These observations were consistent throughout the three times of the day and across the 10 studied cities.
- Comparing in-car $PM_{2.5}$ and PM_{10} levels across cities, African and Asian cities along with CAI can be grouped as showing higher concentrations than those of Latin American cities and SUL, which experience lower PM concentrations. There is a negative correlation (exponential decay) between in-car $PM_{2.5}$ concentrations and city-specific GDP per capita, where countries with low GDP showed high levels of in-car exposure, suggesting social injustice. CAN was an exception to this trend, which demonstrates that ambient air pollution control efforts are not keeping up with economic development. It was also noted

that car population in a city does not necessarily mean higher PM exposure and that other factors (e.g. vehicle fuel/technology, urban layout, green areas throughout the route, the local legislation and city-specific conditions) are significant. For example, ADD had less than one-fifth of SAO's car count but in-car $PM_{2.5}$ and PM_{10} concentrations in ADD were 72% and 82% higher than in SAO.

- Subtraction of recirculation setting concentrations, representing in-car background PM levels, from fan-on and windows-open concentrations, gave an estimate of increased in-car PM concentrations caused by ingress of outdoor pollutants from different sources in each city. The resulting concentration variations for in-car $PM_{2.5}$ and PM_{10} concentrations for windows-open and fan-on show that, irrespective of city and car model, in-car filters are more effective in removing coarse particles than fine particles. This indicates a need for future cars to deploy improved filtration technologies to effectively remove fine particles.

- The benefit of commuting outside peak hours was also reinforced across most cities. For example, most cities (except DAC, CHE and BLZ) showed ratios of MP/OP >EP/OP, indicating higher $PM_{2.5}$ exposure during MP than at any other period. A few cities (DAC and CHE) showed the ratio of MP/OP and EP/OP as ~1, indicating no differences in commuting during peak or off-peak hours.

- A $PM_{2.5}/PM_{10}$ ratio of >0.5 during recirculation and fan-on indicates dominance of fine particles during these settings. During windows-open, CAI and DAR showed $PM_{2.5}/PM_{10}$ <0.5, suggesting a dominance of coarse particles due to arid and dry environments. $PM_{2.5}/PM_{10}$ ratios in CAN reach up to 0.9 in some instances, showing the dominance of fine particles, as is common in Chinese cities due to rapid industrial and economic advancements.

- Spatial variation analysis highlighted pollution hotspots and low-pollution sections along the different routes across the 10 cities. This analysis highlights the factors affecting pollution levels along a route, to help car users in avoiding pollution hotspots and to support policy-makers to introduce pollution mitigation measures at such critical locations in a city.

- The normalisation of concentrations between 0 and 100 allowed us to cross-compare in-car concentrations. Generally, the highest C_{norm} during windows-open verified them to be the worst exposure conditions. Their C_{norm} based categorisation into low (MED, SAO and SUL), intermediate (CAN, CHE, DAC, CAI, ADD and BLZ) and high (DAR) would allow them to understand similarities with other cities in the same group and learn from the strategies adopted by cities in the less polluted groups.

- Increased inhaled doses were found to positively correlate with journey time and in-car concentrations. For instance, higher concentrations during MP lead to increased inhaled doses, whereas an inverse trend was seen during OP, where the time spent and concentrations were less compared with other peak hours. EP was mixed, with higher time spent inside the car (to increase doses) but slightly lower concentrations (to decrease doses) when compared with MP, which explains the resulting doses being in between the other two periods. An inverse correlation between personal exposure and car speed was observed, which was evident in cities like CAN, where in-car concentrations and car speed were up to 2.9-times and 2.5-times higher, respectively, than in MDE and SAO, but these cities showed nearly identical values of inhaled doses.

This study demonstrated an application of affordable laser particle counters for mobile monitoring across 10 cities and built a first global dataset of in-car PM exposure. We showed that exposure concentrations vary with the choice of car setting, period of the day, route characteristics and city-specific conditions like urban layout, meteorology, geography and congestion patterns. Fresh fumes from tailpipe emissions result in commuters' exposure to frequent transient peaks in near-road environments. Dylos is an affordable equipment and therefore the accuracy of the data generated is limited. Nevertheless, the dataset is an innovative strategy to provide the first insights on the main determinants of pollution in traffic environments, and does not affect our findings and conclusions since our results are mainly comparisons between locations, settings and periods of the day. Measurements of gaseous pollutants were not made in this study due to practical constraints, such as the availability of similar sets of instruments. Thus, further studies are recommended to assess the concentrations of gaseous pollutants simultaneously for a more holistic assessment. The derived conclusions are specific to the cities, seasons and routes chosen for this study; therefore, further studies are recommended to estimate exposure concentrations based on shorter averaging time for specific segments of each route, to enable quantification of spatial variability in exposure concentrations. Alternative routes between a particular origin and destination pair could be measured to assess whether exposure concentrations in a given setting are sensitive to route choice. Measurements could also be made in other seasons to assess seasonal variability. The design of future studies should consider the micro-assessment of route characteristics and varying exposure times. Assessing the exposure of commuters utilising different modes of transport, including buses, metro, cycling and walking, would offer an even more holistic assessment. Future studies may also consider the quantification of metals and polycyclic aromatic hydrocarbons in aerosol particles, to enable toxicity-based risk assessments.

CRediT authorship contribution statement

Prashant Kumar: Conceptualization, Funding acquisition, Resources, Methodology, Supervision, Project administration, Writing - original draft, Writing - review & editing. **Sarkawt Hama:** Writing - original draft, Data curation, Visualization, Validation, Writing - review & editing. **Thiago Nogueira:** Formal analysis, Data curation, Writing - original draft, Investigation, Validation, Writing - review & editing. **Rana Alaa Abbass:** Writing - original draft, Investigation, Writing - review & editing. **Veronika S. Brand:** Formal analysis, Data curation, Writing - original draft, Investigation, Validation, Writing - review & editing. **Maria de Fatima Andrade:** Writing - review & editing. **Araya Asfaw:** Writing - review & editing. **Kosar Hama Aziz:** Investigation, Writing - review & editing. **Shi-Jie Cao:** Investigation, Writing - review & editing. **Ahmed El-Gendy:** Writing - review & editing. **Shariful Islam:** Investigation. **Farah Jeba:** Investigation. **Mukesh Khare:** Writing - review & editing. **Simon Henry Mamuya:** Investigation. **Jenny Martinez:** Investigation. **Ming-Rui Meng:** Investigation. **Lidia Morawska:** Writing - review & editing. **Adamson S. Muula:** Investigation, Writing - review & editing. **Shiva Nagendra S M:** Investigation, Writing - review & editing. **Aiwerasia Vera Ngowi:** Investigation, Writing - review & editing. **Khalid Omer:** Writing - review & editing. **Yris Olaya:** Investigation, Writing - review & editing. **Philip Osano:** Writing - review & editing. **Abdus Salam:** Writing - review & editing.

Declaration of competing interest

The authors declare no conflict of interest.

Acknowledgements

Appendix A. Supplementary data

Supplementary data to this article can be found online at https://doi.org/10.1016/j.scitotenv.2020.141395.

References

Abbass, R.A., Kumar, P., El-Gendy, A., 2020. Car users exposure to particulate matter and gaseous air pollutants in megacity Cairo. Sustain. Cities Soc. 56, 102090.

Anderson, J.O., Thundiyil, J.G., Stolbach, A., 2012. Clearing the air: a review of the effects of particulate matter air pollution on human health. J. Med. Toxicol. 8, 166–175.

Andrade, M.F., Kumar, P., Freitas, E.D., Ynoue, R.Y., Martins, J., Martins, L.D., Nogueira, T., Perez-Martinez, P., Miranda, R.M., Albuquerque, T., Gonçalves, F.L.T., Oyama, B., Zhang, Y, 2017. Air quality in the megacity of São Paulo: Evolution over the last 30 years and future perspectives. Atmospheric Environment 159, 66–82. https://doi.org/10.1016/j.atmosenv.2017.03.051.

Anenberg, S.C., Achakulwisut, P., Brauer, M., Moran, D., Apte, J.S., Henze, D.K., 2019. Particulate matter-attributable mortality and relationships with carbon dioxide in 250 urban areas worldwide. Sci. Rep. 9, 11552.

Área Metropolitana del Valle de Aburrá (AMVA), 2017. Plan Integral de Gestión de la Calidad del Aire para el Área Metropolitana del Valle de Aburrá (PIGECA 2017-2030). https://www.medellincomovamos.org/download/plan-integral-de-gestion-de-la-calidad-del-aire-pigeca/. (Accessed 19 March 2020).

Área Metropolitana del Valle de Aburrá (AMVA), 2019. Plan de Acción para la Implementación del Plan Operacional para Enfrentar Episodios de Contaminación Atmosférica (POECA) en el Área Metropolitana del Valle de Aburrá. https://www.metropol.gov.co/ambiental/calidad-del-aire/Documents/POECA/Plan_de_Acci%C3%B3n_POECA_Metropolitano_2019.pdf. (Accessed 19 March 2020).

Betancourt, M.R., Galvis, B., Balachandran, S., Ramos-Bonilla, J.P., Sarmiento, O.L., Gallo-Murcia, S.M., Contreras, Y., 2017. Exposure to fine particulate, black carbon, and particle number concentration in transportation microenvironments. Atmos. Environ. 157, 135–145.

Brand, V.S., Kumar, P., Damascena, A.S., Pritchard, J.P., Geurs, K.T., Andrade, M.F., 2019. Impact of route choice and period of the day on cyclists' exposure to black carbon in London, Rotterdam and São Paulo. J. Transp. Geogr. 76, 153–165.

Brauer, M., Lencar, C., Tamburic, L., Koehoorn, M., Demers, P., Karr, C., 2008. A cohort study of traffic-related air pollution impacts on birth outcomes. Environ. Health Perspect. 116, 680–686.

Brugge, D., Durant, J.L., Rioux, C., 2007. Near-highway pollutants in motor vehicle exhaust: a review of epidemiologic evidence of cardiac and pulmonary health risks. Environ. Health 6, 23.

Carslaw, D.C., Ropkins, K., 2012. openair — an R package for air quality data analysis. Environ. Model Softw. 27-28, 52–61.

Carvlin, G.N., Lugo, H., Olmedo, L., Bejarano, E., Wilkie, A., Meltzer, D., Wong, M., King, G., Northcross, A., Jerrett, M., English, P.B., Hammond, D., Seto, E., 2017. Development and field validation of a community-engaged particulate matter air quality monitoring network in Imperial, California, USA. J. Air Waste Manage. Assoc. 67, 1342–1352.

Cepeda, M., Schoufour, J., Freak-Poli, R., Koolhaas, C.M., Dhana, K., Bramer, W.M., Franco, O.H., 2017. Levels of ambient air pollution according to mode of transport: a systematic review. Lancet Public Health 2, e23–e34.

Davis, S.C., Boundy, R.G., 2016. Transportation Energy Data Book. 37th ed. Oak Ridge National Laboratory for the U.S. Department of Energy's Office of Energy Vehicle Technologies Office https://tedb.ornl.gov. (Accessed 1 December 2019).

Do, D.H., Van Langenhove, H., Chigbo, S.I., Amare, A.N., Demeestere, K., Walgraeve, C., 2014. Exposure to volatile organic compounds: comparison among different transportation modes. Atmos. Environ. 94, 53–62.

Dons, E., Int Panis, L., Van Poppel, M., Theunis, J., Wets, G., 2012. Personal exposure to Black Carbon in transport microenvironments. Atmos. Environ. 55, 392–398.

Gdstats, 2017. China NBS/Bulletin on Reforming Guangdong's GDP Accounting and Data Release System. gdstats.gov.cn (9-Dec-17).

Goel, A., Kumar, P., 2014. A review of fundamental drivers governing the emissions, dispersion and exposure to vehicle-emitted nanoparticles at signalised traffic intersections. Atmos. Environ. 97, 316–331.

Goel, A., Kumar, P., 2015. Characterisation of nanoparticle emissions and exposure at traffic intersections through fast-response mobile and sequential measurements. Atmos. Environ. 107, 374–390.

Ham, W., Vijayan, A., Schulte, N., Herner, J.D., 2017. Commuter exposure to PM2.5, BC, and UFP in six common transport microenvironments in Sacramento, California. Atmos. Environ. 167, 335–345.

Hama, S.M., Kumar, P., Harrison, R.M., Bloss, W.J., Khare, M., Mishra, S., Namdeo, A., Sokhi, R., Goodman, P., Sharma, C., 2020. Four-year assessment of ambient particulate matter and trace gases in the Delhi-NCR region of India. Sustain. Cities Soc. 54, 102003.

Han, I., Symanski, E., Stock, T.H., 2017. Feasibility of using low-cost portable particle monitors for measurement of fine and coarse particulate matter in urban ambient air. J. Air Waste Manage. Assoc. 67, 330–340.

Han, L.J., Zhou, W.Q., Li, W.F., Qian, Y.G., Wang, W.M., 2019. Fine particulate (PM2.5) dynamics before and after China's "Reform and Opening up" policy in Shenzhen. Phys. Chem. Earth 111, 100–104.

Hasenkopf, C.A., Adukpo, D.C., Brauer, M., Dewitt, H.L., Guttikunda, S., Alaa, I., Ibrahim, A.I., Lodoisamba, D., Mutanyi, N., Olivares, G., Pant, P., Salmon, M., Sereeter, L., 2016. To combat air inequality, governments and researchers must open their data. Clean Air Journal 26, 8–10.

HEI, 2010. Traffic-related Air Pollution: A Critical Review of the Literature on Emissions, Exposure, and Health Effects. Health Effects Institute, Boston, MA https://www.healtheffects.org/publication/traffic-related-air-pollution-critical-review-literature-emissions-exposure-and-health. (Accessed 1 December 2019).

Hertel, O., Hvidberg, M., Ketzel, M., Storm, L., Stausgaard, L., 2008. A proper choice of route significantly reduces air pollution exposure—a study on bicycle and bus trips in urban streets. Sci. Total Environ. 389, 58–70.

Hinds, W.C., 1999. Aerosol Technology: Properties, Behaviour and Measurement of Airborne Particles. John Wiley & Sons, UK, p. 483.

Holstius, D.M., Pillarisetti, A., Smith, K.R., Seto, E., 2014. Field calibrations of a low-cost aerosol sensor at a regulatory monitoring site in California. Atmos. Meas. Tech. 7, 1121–1131.

Jiao, W., Hagler, G., Williams, R., Sharpe, R., Brown, R., Garver, D., Judge, R., Caudill, M., Rickard, J., Davis, M., Weinstock, L., Zimmer-Dauphinee, S., Buckley, K., 2016. Community Air Sensor Network (CAIRSENSE) project: evaluation of low-cost sensor performance in a suburban environment in the southeastern United States. Atmos. Meas. Tech. 9, 5281–5292.

Jung, H.S., Grady, M.L., Victoroff, T., Miller, A.L., 2017. Simultaneously reducing CO2 and particulate exposures via fractional recirculation of vehicle cabin air. Atmos. Environ. 160, 77–88.

Kioumourtzoglou, M.A., Schwartz, J.D., Weisskopf, M.G., Melly, S.J., Wang, Y., Dominici, F., Zanobetti, A., 2016. Long-term PM2.5 exposure and neurological hospital admissions in the northeastern United States. Environ. Health Perspect. 124, 23–29.

Kollanus, V., Prank, M., Gens, A., Soares, J., Vira, J., Kukkonen, J., Sofiev, M., Salonen, R.O., Lanki, T., 2017. Mortality due to vegetation fire–originated PM 2.5 exposure in Europe—assessment for the years 2005 and 2008. Environ. Health Perspect. 125, 30–37.

Kumar, P., Goel, A., 2016. Concentration dynamics of coarse and fine particulate matter at and around signalised traffic intersections. Environ Sci Process Impacts 18, 1220–1235.

Kumar, P., Imam, B., 2013. Footprints of air pollution and changing environment on the sustainability of built infrastructure. Sci. Total Environ. 444, 85–101.

Kumar, P., Khare, M., Harrison, R.M., Bloss, W.J., Lewis, A., Coe, H., Morawska, L., 2015a. New directions: air pollution challenges for developing megacities like Delhi. Atmos. Environ. 122, 657–661.

Kumar, P., Morawska, L., Martani, C., Biskos, G., Neophytou, M., Di Sabatino, S., Bell, M., Norford, L., Britter, R., 2015b. The rise of low-cost sensing for managing air pollution in cities. Environ. Int. 75, 199–205.

Kumar, P., Andrade, M.F., Ynoue, R.Y., Fornaro, A., de Freitas, E.D., Martins, J., Martins, L.D., Albuquerque, T., Zhang, Y., Morawska, L., 2016. New directions: from biofuels to wood stoves: the modern and ancient air quality challenges in the megacity of São Paulo. Atmos. Environ. 140, 364–369.

Kumar, P., Rivas, I., Sachdeva, L., 2017. Exposure of in-pram babies to airborne particles during morning drop-in and afternoon pick-up of school children. Environ. Pollut. 224, 407–420.

Kumar, P., Patton, A.P., Durant, J.L., Frey, H.C., 2018a. A review of factors impacting exposure to PM2.5, ultrafine particles and black carbon in Asian transport microenvironments. Environ. 187, 301–316.

Kumar, P., Rivas, I., Singh, A.P., Ganesh, V.J., Ananya, M., Frey, H.C., 2018b. Dynamics of coarse and fine particle exposure in transport microenvironments. npj Climate Atmos. Sci. 1 (1), 1–12. https://doi.org/10.1038/s41612-018-0023-y.

Landrigan, P.J., Fuller, R., Acosta, N.J.R., Adeyi, O., Arnold, R., Basu, N., Baldé, A.B., Bertollini, R., Bose-O'Reilly, S., Boufford, J.I., Breysse, P.N., Chiles, T., Mahidol, C., Coll-Seck, A.M., Cropper, M.L., Fobil, J., Fuster, V., Greenstone, M., Haines, A., Hanrahan, D., Hunter, D., Khare, M., Krupnick, A., Lanphear, B., Lohani, B., Martin, K., Mathiasen, K.V., McTeer, M.A., Murray, C.J.L., Ndahimananjara, J.D., Perera, F., Potočnik, J., Preker, A.S., Ramesh, J., Rockström, J., Salinas, C., Samson, L.D., Sandilya, K., Sly, P.D., Smith, K.R., Steiner, A., Stewart, R.B., Suk, W.A., van Schayck, O.C.P., Yadama, G.N., Yumkella, K., Zhong, M., 2018. The Lancet Commission on pollution and health. Lancet 391, 462–512.

Lelieveld, J., Evans, J.S., Fnais, M., Giannadaki, D., Pozzer, A., 2015. The contribution of outdoor air pollution sources to premature mortality on a global scale. Nature 525, 367.

Lelieveld, J., Pozzer, A., Pöschl, U., Fnais, M., Haines, A., Münzel, T., 2020. Loss of life expectancy from air pollution compared to other risk factors: a worldwide perspective. Cardiovasc. Res. https://doi.org/10.1093/cvr/cvaa025.

Li, X., Chen, X., Yuan, X., Zeng, G., León, T., Liang, J., Chen, G., Yuan, X., 2017a. Characteristics of particulate pollution (PM2.5 and PM10) and their spacescale-dependent relationships with meteorological elements in China. Sustainability 9 (12), 2330.

Li, Z., Che, W., Frey, H.C., Lau, A.K.H., Lin, C., 2017b. Characterization of PM2.5 exposure concentration in transport microenvironments using portable monitors. Environ. Pollut. 228, 433–442.

Lim, M., Myagmarchuluun, S., Ban, H., Hwang, Y., Ochir, C., Lodoisamba, D., Lee, K., 2018. Characteristics of indoor PM2.5 concentration in Gers using coal stoves in Ulaanbaatar, Mongolia. Int. J. Environ. Res. Public Health 15, 1–11.

Loxham, M., Nieuwenhuijsen, M.J., 2019. Health effects of particulate matter air pollution in underground railway systems – a critical review of the evidence. Part. Fibre Toxicol. 16 (1).

Malley, C.S., Braban, C.F., Heal, M.R., 2014. The application of hierarchical cluster analysis and non-negative matrix factorization to European atmospheric monitoring site classification. Atmos. Res. 138, 30–40.

Manikonda, A., Zíková, N., Hopke, P.K., Ferro, A.R., 2016. Laboratory assessment of low-cost PM monitors. J. Aerosol Sci. 102, 29–40.

Mapoma, H.W.T., Tsakama, M., Kosamu, I.B.M., 2014. Air quality assessment of carbon monoxide, nitrogen dioxide and sulfur dioxide levels in Blantyre, Malawi: a statistical approach to a stationary environmental monitoring station. African J. Environ. Sci. Technol. 8, 330–343.

Marlier, M.E., Jina, A.S., Kinney, P.L., DeFries, R.S., 2016. Extreme air pollution in global megacities. Curr. Clim. Chang. Reports 2, 15–27.

Mitchell, C.P., Branfireun, B.A., Kolka, R.K., 2008. Spatial characteristics of net methylmercury production hot spots in peatlands. Environ. Sci. Technol. 42 (4), 1010–1016.

MOP, 2019. The Ministry of Planning. http://www.mop.gov.krd/index.jsp. (Accessed 19 March 2020).

Moreira, C.A.B., Squizzato, R., Beal, A., Almeida, D.S., Rudke, A.P., Ribeiro, M., Andrade, M.F., Kumar, P., Martins, L.D., 2018. Natural variability in exposure to fine particles and their trace elements during typical workdays in an urban area. Transp. Res., Part D 63, 333–346.

Nogueira, T., Kumar, P., Nardocci, A., Andrade, M.F., 2020. Public health implications of particulate matter inside bus terminals in Sao Paulo, Brazil. Sci. Total Environ. 711, 135064.

Northcross, A.L., Edwards, R.J., Johnson, M.A., Wang, Z.-M., Zhu, K., Allen, T., Smith, K.R., 2013. A low-cost particle counter as a realtime fine-particle mass monitor. Environ Sci Process Impacts 15, 433–439.

Oliveira, M., Slezakova, K., Delerue-Matos, C., Pereira, M.C., Morais, S., 2019. Children environmental exposure to particulate matter and polycyclic aromatic hydrocarbons and biomonitoring in school environments: a review on indoor and outdoor exposure levels, major sources and health impacts. Environ. Int. 124, 180–204.

Onat, B., Şahin, Ü.A., Uzun, B., Akın, Ö., Özkaya, F., Ayvaz, C., 2019. Determinants of exposure to ultrafine particulate matter, black carbon, and PM2.5 in common travel modes in Istanbul. Atmos. Environ. 206, 258–270.

Panis, L.I., de Geus, B., Vandenbulcke, G., Willems, H., Degraeuwe, B., Bleux, N., Mishra, V., Thomas, I., Meeusen, R., 2010. Exposure to particulate matter in traffic: a comparison of cyclists and car passengers. Atmos. Environ. 44, 2263–2270.

Pant, P., Harrison, R.M., 2013. Estimation of the contribution of road traffic emissions to particulate matter concentrations from field measurements: a review. Atmos. Environ. 77, 78–97.

Petkova, E.P., Jack, D.W., Volavka-Close, N.H., Kinney, P.L., 2013. Particulate matter pollution in African cities. Air Qual. Atmos. Hlth. 6 (3), 603–614.

Quan, J., Gao, Y., Zhang, Q., Tie, X., Cao, J., Han, S., Meng, J., Chen, P., Zhao, D., 2013. Evolution of planetary boundary layer under different weather conditions, and its impact on aerosol concentrations. Particuology 11, 34–40.

Querol, X., Tobías, A., Pérez, N., Karanasiou, A., Amato, F., et al., 2019. Monitoring the impact of desert dust outbreaks for air quality for health studies. Environ. Int. 130, 104867.

R Core Team, 2019. R: A Language and Environment for Statistical Computing. R Foundation for Statistical Computing, Vienna, Austria https://www.R-project.org/.

Rivas, I., Kumar, P., Hagen-Zanker, A., 2017. Exposure to air pollutants during commuting in London: are there inequalities among different socio-economic groups? Environ. Int. 101, 143–157.

Semple, S., Ibrahim, A.E., Apsley, A., Steiner, M., Turner, S., 2015. Using a new, low-cost air quality sensor to quantify second-hand smoke (SHS) levels in homes. Tob. Control. 24, 153–158.

Shaker, R.R., 2018. A mega-index for the Americas and its underlying sustainable development correlations. Ecol. Indic. 89, 466–479.

Smith, M.N., 2016. The number of cars worldwide is set to double by 2040. World Economic Forum https://www.weforum.org/agenda/2016/04/the-number-of-cars-worldwide-is-set-to-double-by-2040. (Accessed 1 December 2019).

Steinle, S., Reis, S., Sabel, C.E., Semple, S., Twigg, M.M., Braban, C.F., Leeson, S.R., Heal, M.R., Harrison, D., Lin, C., Wu, H., 2015. Personal exposure monitoring of PM2.5 in indoor and outdoor microenvironments. Sci. Total Environ. 508, 383–394.

TYCB, 2020. The China Year Book. Available from. http://www.stats.gov.cn/tjsj/ndsj/. (Accessed 13 July 2020).

United Nations, 2018. The World's Cities in 2018-Data Booklet (ST/ESA/ SER.A/417). Department of Economic and Social Affairs, Population Division https://www.un.org/en/events/citiesday/assets/pdf/the_worlds_cities_in_2018_data_booklet.pdf. (Accessed 6 May 2020).

US Environmental Protection Agency, 1992. Guidelines for exposure assessment. Risk assess. forum. http://ofmpub.epa.gov/eims/eimscomm.getfile?p_download_id=429103. (Accessed 12 November 2019).

Wang, N., Ling, Z., Deng, X., Deng, T., Lyu, X., Li, T., Gao, X., Chen, X., 2018. Source contributions to PM2.5 under unfavorable weather conditions in Guangzhou City, China. Adv. Atmos. Sci. 35 (9), 1145–1159.

WHO, 2006. Health Risks of Particulate Matter from Long-range Transboundary Air Pollution. European Centre for Environment and Health, Bonn, Germany http://www.euro.who.int/__data/assets/pdf_file/0006/78657/E88189.pdf. (Accessed 12 November 2019).

WHO, 2016. World Health Organization: AAP Air Quality Database. available at. http://www.who.int/phe/health_topics/outdoorair/databases/cities/en/. (Accessed 21 November 2018).

Yang, F., Kaul, D., Wong, K.C., Westerdahl, D., Sun, L., Ho, K.-f., Tian, L., Brimblecombe, P., Ning, Z., 2015. Heterogeneity of passenger exposure to air pollutants in public transport microenvironments. Atmos. Environ. 109, 42–51.

Yu, Q., Lu, Y., Xiao, S., Shen, J., Li, X., Ma, W., Chen, L., 2012. Commuters' exposure to PM1 by common travel modes in Shanghai. Atmos. Environ. 59, 39–46.

Yuchi, W., Gombojav, E., Boldbaatar, B., Galsuren, J., Enkhmaa, S., Beejin, B., Naidan, G., Ochir, C., Legtseg, B., Byambaa, T., Barn, P., Henderson, S.B., Janes, C.R., Lanphear, B.P., McCandless, L.C., Takaro, T.K., Venners, S.A., Webster, G.M., Allen, R.W., 2019. Evaluation of random forest regression and multiple linear regression for predicting indoor fine particulate matter concentrations in a highly polluted city. Environ. Pollut. 245, 746–753.

Zhang, Y., Gu, Z., 2013. Air quality by urban design. Nat. Geosci. 6 (7), 506.

Zhang, J., Mauzerall, D.L., Zhu, T., Liang, S., Ezzati, M., Remais, J.V., 2010. Environmental health in China: progress towards clean air and safe water. Lancet 375, 1110–1119.

Zhao, D., Chen, H., Yu, E., Luo, T., 2019. PM2.5/PM10 ratios in eight economic regions and their relationship with meteorology in China. Adv. Meteorol. 2019, 1–15.

Zuurbier, M., Hoek, G., Oldenwening, M., Lenters, V., Meliefste, K., van den Hazel, P., Brunekreef, B., 2010. Commuters' exposure to particulate matter air pollution is affected by mode of transport, fuel type, and route. Environ. Health Perspect. 118, 783–789.